Journal of Medicinal Chemistry

pubs.acs.org/jmc

Article

Rebamipide and Derivatives are Potent, Selective Inhibitors of Histidine Phosphatase Activity of the Suppressor of T Cell Receptor Signaling Proteins

Faisal Aziz,[⊥] Kanamata Reddy,[⊥] Virneliz Fernandez Vega, Raja Dey, Katherine A. Hicks, Sumitha Rao, Luis Ortiz Jordan, Emery Smith, Justin Shumate, Louis Scampavia, Nicholas Carpino, Timothy P. Spicer, and Jarrod B. French*

Cite This: *J. Med. Chem.* 2024, 67, 1949−1960

Read Online

ACCESS | Metrics & More | Article Recommendations | Supporting Information

ABSTRACT: The suppressor of T cell receptor signaling (Sts) proteins are negative regulators of immune signaling. Genetic inactivation of these proteins leads to significant resistance to infection. From a 590,000 compound high-throughput screen, we identified the 2-(*1H*)-quinolinone derivative, rebamipide, as a putative inhibitor of Sts phosphatase activity. Rebamipide, and a small library of derivatives, are competitive, selective inhibitors of Sts-1 with IC_{50} values from low to submicromolar. SAR analysis indicates that the quinolinone, the acid, and the amide moieties are all essential for activity. A crystal structure confirmed the SAR and reveals key interactions between this class of compound and the protein. Although rebamipide has poor cell permeability, we demonstrated that a liposomal preparation can inactivate the phosphatase activity of Sts-1 in cells. These studies demonstrate that Sts-1 enzyme activity can be pharmacologically inactivated and provide foundational tools and insights for the development of immune-enhancing therapies that target the Sts proteins.

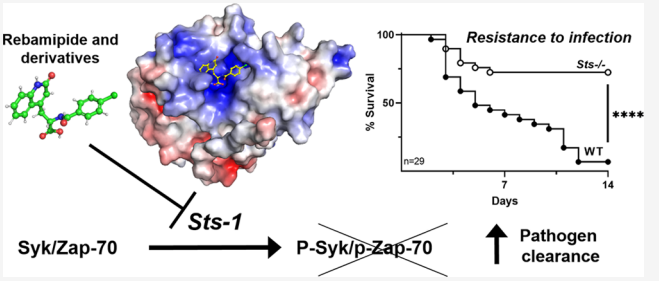

INTRODUCTION

The suppressor of T cell receptor signaling (Sts) proteins are a pair of multidomain phosphatases that are 50% sequence identical and have overlapping, redundant functions.[1] These proteins act as negative regulators of signaling pathways downstream of the T cell receptor complex.[1,2] Genetic inactivation of Sts-1 and Sts-2 in mice ($Sts^{-/-}$) leads to resistance to systemic infection by a broad range of pathogens including the fungus *C. albicans* as well as both Gram-positive and Gram-negative bacteria.[3] In addition to enhanced survival, the resistance phenotype is characterized by rapid pathogen clearance, an altered inflammatory response, and a lack of deleterious immunopathology.[3a,4] Further analysis of the two homologous proteins has revealed that Sts-1, which has a significantly higher phosphatase activity, plays the predominant role, and in most cases, inactivation of Sts-1 alone yields a resistance phenotype similar to that of the double knockout.[5] These studies suggest that functional inactivation of Sts-1 could yield important clinical benefits that are broadly applicable to the treatment of systemic infections by bacterial and fungal pathogens.

Sts-1 (also called TULA-2 or UBASH3B) and Sts-2 (also called TULA-1 or UBASH3A) share a unique domain organization composed of a C-terminal histidine phosphatase (HP) domain,[1,5a] an internal region recently identified as a cyclic nucleotide phosphodiesterase (PDE),[6] and two protein−protein interacting domains, namely, ubiquitin associating (UBA) and src-homology 3 (SH3) domains. The predominant means by which the Sts proteins are known to regulate immune signaling pathways is through the activity catalyzed by the HP domain. This domain has been demonstrated, through a variety of genetic, cellular, and biochemical approaches, to be a protein tyrosine phosphatase (PTP) that dephosphorylates the kinases Syk and Zap-70.[2b,5a,b,7] Although the Sts proteins are PTPs, they are structurally distinct from canonical PTPs, such as PTP-1B, and lack the conserved active site C(X)5R PTP signature motif. The protein fold of the HP domain of Sts is more similar to bacterial phosphoglycerate mutase (PGM), an isomerase that transfers a phosphate group from the C-3 to C-2 position on glycerol during glycolysis.[5a,c,8] Also unlike other PTPs, the HP domain of the Sts enzymes employs a distinct enzymatic mechanism to dephosphorylate phosphotyrosine substrates. These enzymes have two conserved active site

Received: September 22, 2023
Revised: December 8, 2023
Accepted: December 29, 2023
Published: January 22, 2024

histidine residues and are proposed to follow a mechanism, similar to other histidine phosphatases, that proceeds through a covalent phospho-histidine intermediate.[9]

The observed resistance phenotype resulting from Sts knockdown, combined with an active site that is structurally distinct from other PTPs, makes the HP domain of Sts an attractive drug target for the development of small molecule antimicrobials. Despite this opportunity, little progress has been made toward the development of Sts inactivators. Prior studies have yielded nonspecific PTP inhibitors, low activity compounds, and nondrug-like hits.[5c,10] While these demonstrate the druggability of the protein, they do not provide a clear direction for further development nor a foundation upon which to build a lead series. To identify novel inhibitors of the HP activity of Sts-1 (Sts-1_{HP}), we recently conducted a 590,000 compound high-throughput screen at The Molecular Screening Center at UF Scripps.[11] Among the top hits in this screen was the known antiulcer drug rebamipide. We generated a small library of rebamipide analogs and determined that these compounds are selective, competitive inhibitors of Sts-1_{HP} with IC_{50} values ranging from low to sub-μM. To further support this structure activity (SAR) work, we also solved X-ray cocrystal structures of rebamipide and one derivative. These results established a binding mode that is consistent with observed SAR data. Not surprisingly, while rebamipide was active against the Sts-1_{HP} enzyme, little or no activity was observed in cell-based assays. However, when the compound was delivered to cells in liposomes, inhibition of Sts-1 dephosphorylation of Zap-70 was clearly observed. Together, these results describe an active series of Sts-1_{HP} inhibitors with potential for further development if limitations to cell permeability can be overcome.

RESULTS AND DISCUSSION

High-Throughput Screening to Identify Inhibitors of Sts-1_{HP}. We previously determined that the isolated HP domain of Sts-1 (Sts-1_{HP}) has an equivalent phosphatase activity as that of the full-length protein, is much more amenable to purification and handling, and behaves well in 1,536-well plate format screening assays.[10b] Using our established assays,[5a,c,10b] we completed a screen of 590,748 compounds of the complete Scripps Drug Discovery Library using Sts-1_{HP}. The assay performed well, with an average signal-to-background (S:B) of 12.71 ± 1.26 (n = 475 plates) and an average Z' of 0.87 ± 0.04. Controls included a high control (no enzyme activity) with substrate but lacking enzyme, low control with substrate, enzyme and vehicle only (DMSO, full enzyme activity), and reference control using the nonspecific Sts-1_{HP} inhibitor PHPS1.[5c,10b,12] An interval cutoff of 16.43%, defined as the average percent inhibition of all compounds between the low control and high control values plus three times the standard deviation of this value, was used to select 7,879 compounds. A promiscuity index was also calculated using former UF Scripps HTS data and represents the number of times that a compound was observed as a hit over the number of times that compound was used in a primary screen. The selected compounds were also evaluated for obvious pan assay interference compounds (PAINS).[13] Of the 7,879 compounds, 5,873 with a promiscuity value ≤5 and no PAINS issues were selected for secondary assays. A counterscreen assay was completed by running the same assay on the cherry-picked compounds at a single concentration (5.8 μM) in triplicate and repeating this procedure but adding the compounds after the assay quenching step. A primary assay confirmation was also completed using the same triplicate format, and high activity in both assays was considered as possible quenchers or artifacts of the assay. From these assays, 125 compounds appeared to be active only in the primary screen. A 10-point titration assay (3-fold dilution series) was carried out with these compounds, and percent response was plotted against compound concentration. A four-parameter equation describing a sigmoidal dose−response curve was used fit to the data to generate IC_{50} values (Symyx Technologies, Inc.). All compounds selected for titration were analyzed by LC−MS to confirm purity and mass.

Rebamipide Competitively Inhibits the Phosphatase Activity of Sts-1. The known antiulcerative drug rebamipide was found within the top hits identified in the screen and one of only three hits with a promiscuity value of 1 (this was the first time this compound had been confirmed as a hit in over 100 screens conducted) (Figure 1A). Rebamipide is an amino

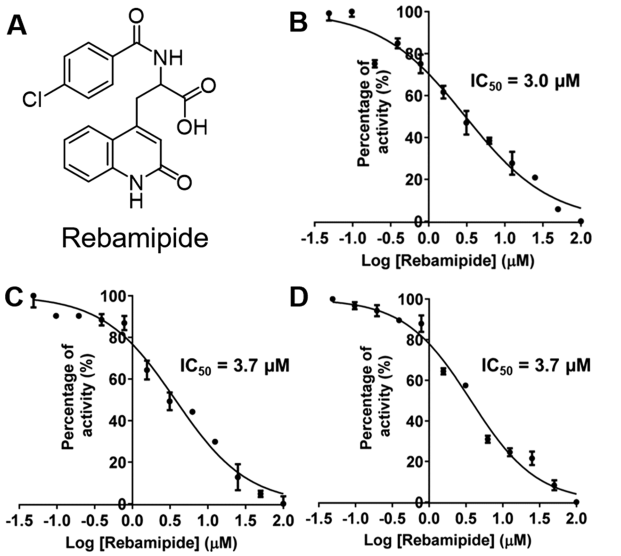

Figure 1. Rebamipide inhibits the PTP activity of Sts-1. The known antiulcerative, Rebampide (A), was identified in a HTS screen. This compound shows consistent, substrate-independent activity, for multiple PTP substrates including pNPP (B), OMFP (C), and DiFMUP (D). Data shown are the mean of triplicate measurements ± standard error.

acid derivative of 2-(*1H*)-quinolinone that is clinically approved for use in a number of countries in Asia for mucosal protection and treatment of ulcers.[14] The IC_{50} of rebamipide was 3 μM when using pNPP (1 mM, K_M = 2.6 mM) as a substrate or 3.7 μM when using OMFP (150 μM, K_M = 190 μM) or DiFMUP (1.5 μM, K_M = 2 μM) as substrates (Figures 1B−D). To determine the mechanism of action, we compared the kinetics of Sts-1_{HP}, using two different assays, in the presence of increasing concentrations of rebamipide (Figure 2). The compound appears to impact the K_M only, suggesting that it is a competitive inhibitor with a K_i of 2 μM. Lineweaver−Burk plots (Figure S1) of the data are also consistent with competitive inhibition. To confirm that the compound is competing with the substrate in the active site, we also tested an active site mutant of Sts-$1_{HP,}$ W505L, that alters the nature of the active site but does not eliminate enzyme activity.[10b] When this tryptophan is changed to a leucine residue, rebamipide loses its activity and is unable to

https://doi.org/10.1021/acs.jmedchem.3c01763
J. Med. Chem. 2024, 67, 1949−1960

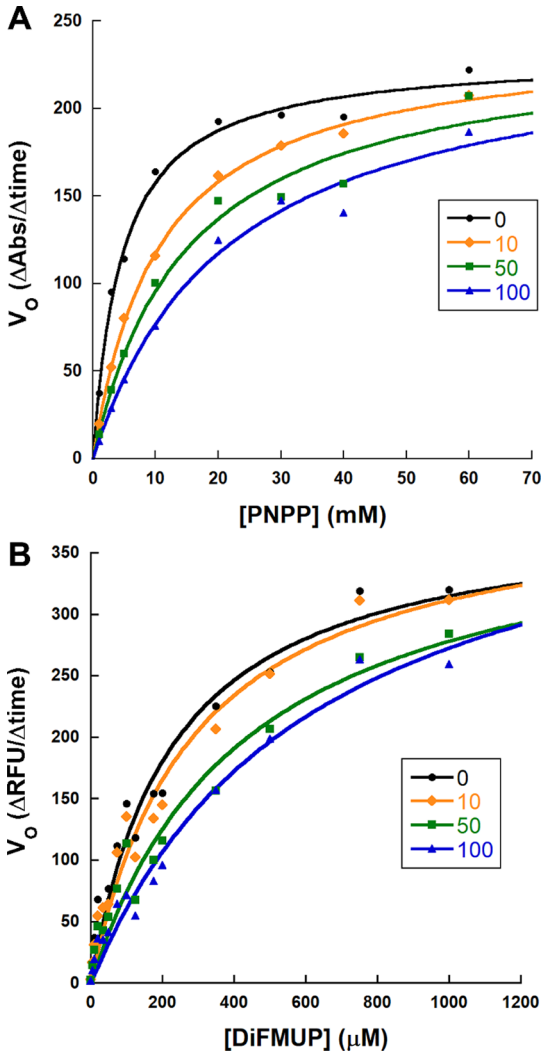

Figure 2. Rebamipide is a competitive inhibitor of Sts-1_{HP}. Increasing rebamipide concentrations lower the K_M of the reaction catalyzed by Sts-1_{HP}. Data shown are the substrates pNPP (A) and DiFMUP (B). The Lineweaver–Burk plot of this data is shown in Figure S1.

inhibit the enzyme (Figure S2). Taken together with our kinetic data and the structural information provided below, this data is consistent with rebamipide acting as a competitive inhibitor that makes critical interactions with the active site tryptophan.

Initial SAR Studies. To determine which features of rebamipide make important contributions to its inhibitory activity against Sts-1, we synthesized a small library of analogs (Figure 3). Using the pNPP assay, we determined the activity of these compounds against Sts-1 (Figure 3). From these data, we observed several trends. No activity was observed when quinolinone was removed or substituted with an indole (**2**) or naphthyl (**3**). A prior study indicated that highly functionalized planar aromatics, such as teracyclines or azo dyes, were able to act as competitive inhibitors.[10b] This work pointed to an interaction with the active site tryptophan, W494, as the main driver of this observation. We also observed that the acid and backbone amide also appeared to be important for overall activity. Changing the acid to an ester (**29**) or hydroxamic acid (**30**) yielded an inactive compound. Attempts to increase the linker length between the quinolinone and the phenyl group also failed to improve activity (**27, 32, 33, and 34**). The terminal phenyl group was relatively tolerant to substitution of the chlorine by various groups (**1, 7**–**22**), but the activity decreased moving this group from the *para* > *meta* > *ortho* position (**1,18, and 16**). Surprisingly, the most potent compound identified, with a submicromolar IC_{50}, was a dimeric form of rebamipide formed through an ether linkage on the terminal phenyl (**28**). While the solved structures of the HP domain of Sts-1 suggests that this protein is dimeric, the active sites are greater than 20 Å apart. This would indicate that compound **28** could not engage both active sites at the same time. This suggests that additional structural features of the active site, beyond where the phenyl group binds, can be exploited to increase the activity of this class of compound.

Sts-1_{HP}-rebamipide Structure. High resolution crystal structures of the HP domain of Sts-1 have previously been solved for the human and mouse proteins.[5a,c,8a] While these include unliganded as well as sulfate or phosphate bound structures, no ligand-bound form of any Sts HP domain has yet been reported. To better understand how rebamipide binds to, and inhibits, Sts-1 phosphatase activity, we determined a cocrystal structure of Sts-1_{HP} with rebamipide bound (Figures 4 and S3). While the ligand occupancy varies in the six chains of the 2.5 Å crystal structure, clear electron density is visible and corresponds well to the structure of rebamipide. As a further confirmation of this binding mode, we also solved the structure of the *para*-ethyl derivative of rebamipide (**11**, Figure S4). While this latter structure was solved at a lower resolution and is of overall lower quality, the electron density for the ligand confirms the binding mode of the compound. Overall, rebamipide can be seen fitting deeply into the electropositive active site of Sts-1_{HP} (Figure 4A) A closer look at the active site reveals key interactions between Sts-1_{HP} and rebamipide (Figure 4B). The quinolinone group makes an important π-cation stacking interaction with W494 of the protein. This is consistent with our activity data and also the prior observation that planar aromatic molecules tend to be preferred in the active site. Similarly, the phenyl group of rebamipide π-stacks with R383. The importance of this stacking interaction and its position in the active site is observed in the substantial reduction in activity of the difluoro or $-CF_3$ derivatives (**9, 19, and 20**). The binding pocket is mostly open around this group, particularly at the para position, consistent with the relative insensitivity to modifications of the ring at this position (**1, 7**–**22**). The carboxylic acid group points into the binding pocket, near where the phosphate binds, and makes H-bond interactions with R379, R383, and an ordered water molecule. The position of this group appears to be optimal for H-bonding and precludes the substitution at this site by larger groups. Despite the activity data suggesting that it is important for inhibition of Sts-1_{HP}, the amide group does not make any obvious interactions with the protein. It is likely that the amide backbone helps the molecule assume the correct binding geometry. The observed binding geometry of rebamipide is nearly identical to the predicted low energy conformer model of this compound (Figure S5).[15]

Rebamipide Is a Selective Inhibitor of Sts-1 Phosphatase Activity. The overall structure and active site organization of the HP domain of the Sts proteins is distinct from canonical PTPs and is more similar to the PGM family of proteins. While some nonspecific PTP inhibitors can broadly inhibit Sts HP activity as well as other PTPs, the stark differences in active sites suggest that selective inhibition of Sts phosphatase activity is achievable. To determine if rebamipide

https://doi.org/10.1021/acs.jmedchem.3c01763
J. Med. Chem. 2024, 67, 1949−1960

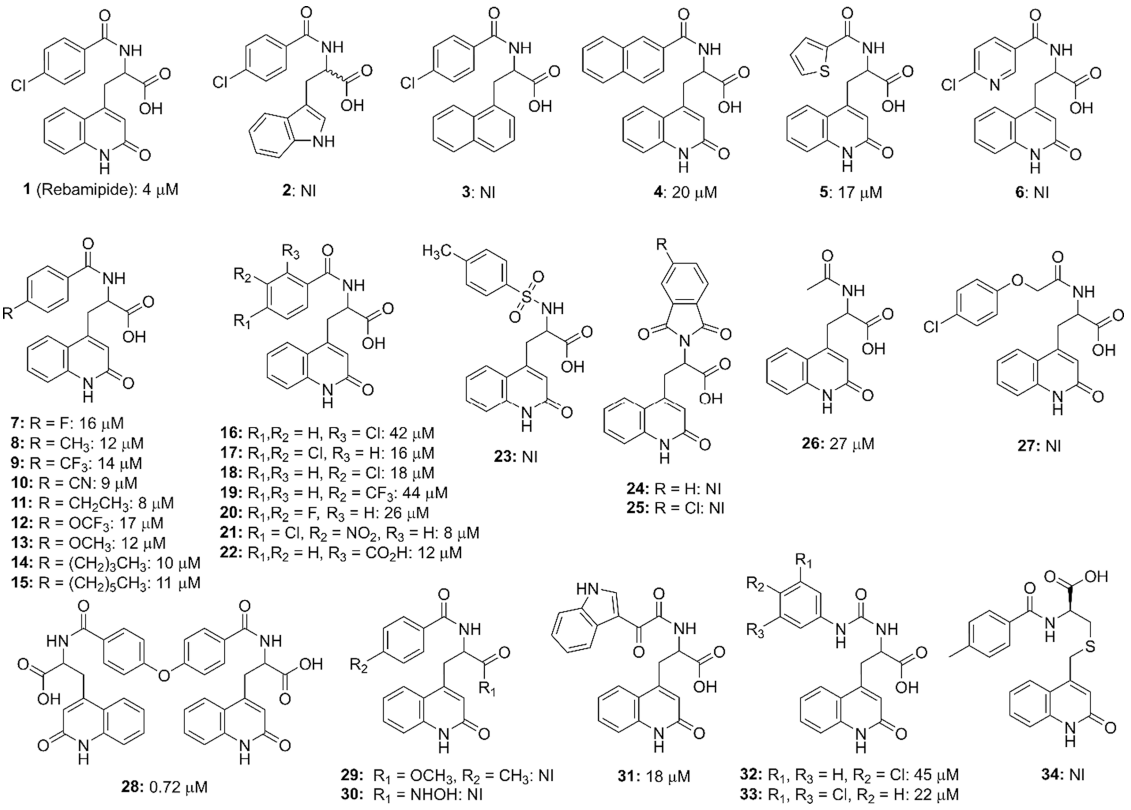

Figure 3. Rebamipide derivatives for initial structure activity relationship studies. The IC_{50} values are given for the small library of compounds synthesized to explore the structure−activity relationship of the activity of this class of compound against Sts-1_{HP}. Error values for the data are included in Table S1.

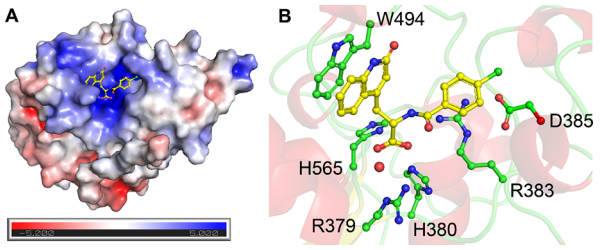

Figure 4. Inhibitor-bound structure of Sts-1_{HP}. Rebamipide occupies the highly basic active site of the phosphastase domain of Sts-1 (A, blue represents higher positive electrostatic potential while red represents higher negative electrostatic potential). A close-up view of the active site (B) shows that rebamipide makes several key interactions with side chains of Sts-1_{HP}, including a π-stacking interaction with W49, hydrogen bonds between the carboxylic acid and both R379 and H380, and π-cation interactions with R383.

shows selectivity for Sts-1_{HP}, we tested two nonreceptor-type PTPs, PTP-1B, and SHP1, and one receptor-type PTP, CD45. We generated dose−response curves, using these enzymes, for rebamipide as well as for the nonspecific PTP inhibitors sodium orthovanadate and PHPS1.[5c,12] As expected, the positive controls, orthovanadate and PHPS1, inhibited the phosphatase activity of all of these enzymes (Figures 5A,B,D,E, S6 and S7). Rebamipide, however, did not show any inhibition of the activity of PTP-1B, SHP1, or CD45 (Figures 5F, S6 and S7). We also determined the effect of rebamipide on Sts-2_{HP}. Rebamipide did inhibit the phosphatse activity of Sts-2, albeit with approximately 2-fold lower IC_{50} (Figure S8). Despite a relatively high degree of structural conservation between Sts-1_{HP} and Sts-2_{HP}, the latter enzyme exhibits much slower kinetics for all substrates tested.[5c,8a] Considering it is broader distribution and larger impact on the resistance phenotype, Sts-1 is predicted to be the more clinically relevant form.[5]

Rebamipide Inhibits Sts PTP Activity in Cells. In order to confirm that rebamipide had activity against Sts in cell culture, we used a previously reported HEK-293T based assay.[5c] However, we were unable to see increased phosphorylation of Zap-70 following treatment of cells with rebamipide (Figure 6, column 4). In contrast, when we delivered rebamipide to the cells in liposomes, we saw a clear increase in phospho-Zap-70 levels indicating inhibition of Sts PTP activity (Figure 6A, columns 6 and 7). Similar results were observed when assayed in T cells (Figure 6B). These results suggest that, in this context, rebamipide can effectively inhibit Sts in cells but has limited cell permeability. This is consistent with previous studies of this compound showing it to be safe overall but having poor physicochemical properties, including low aqueous solubility, permeability, and bioavailability.[16]

CONCLUSIONS

This work describes the discovery that the known antiulcerative compound, rebamipide, and some specific analogs, are effective and selective inhibitors of the PTP activity of Sts-1. Our initial SAR studies, supplemented by X-ray crystal structures, suggest that there are four distinct features of this compound class that are important for activity. These include (1) the 2-(*1H*)-quinolinone, that stacks against the active site tryptophan residue (Figure 7, light blue); (2) a terminal substituted phenyl (Figure 7, purple), which makes cation-π interactions with the guanidine group active site arginine; (3) a

https://doi.org/10.1021/acs.jmedchem.3c01763
J. Med. Chem. 2024, 67, 1949−1960

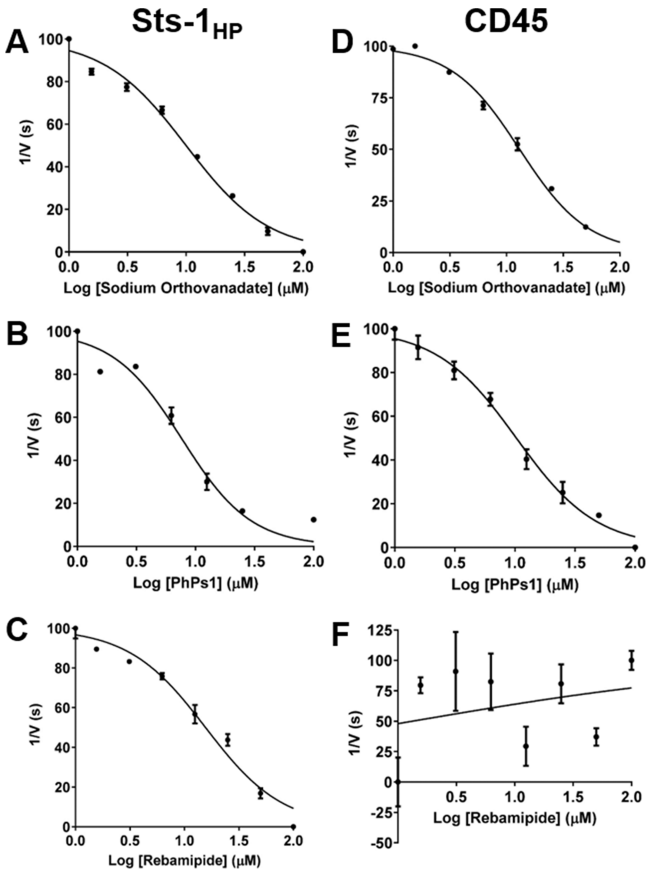

Figure 5. Rebamipide selectively inhibits Sts-1_{HP}. Both of the known nonselective PTP inhibitors, orthovanadate, and PHPS1 inhibit Sts-1_{HP} (A, B) as well as CD45 (D, E). Conversely, while rebamipide inhibits Sts-1 (C), it displays no activity toward CD45 (F). Similar results are seen for other PTPs including PTP-1B (Figure S6) and SHP-2 (Figure S7).

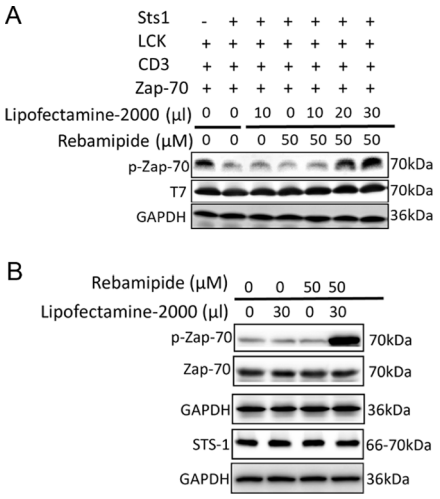

Figure 6. Rebamipide decreases Sts-1 activity in cells when delivered via liposomes. Sts-1 is known to dephosphorylate the kinase Zap-70. Using a cell-based assay, phospho-Zap-70 (p-Zap-70) levels are seen to increase when Sts-1 is absent (A, compare columns 1 to 2). When 50 μM rebamipide is added to cells (A, column 4), no inhibition of Sts-1 is observed, likely owing to the poor cell permeability of rebamipide. However, when rebamipide is delivered to the cells in liposomes (columns 5–7), a high level of p-Zap-70 is observed, indicating that Sts-1 is inhibited. Similar results are seen when using Jurkat cells (B). An increase in p-Zap-70 is seen only when rebamipide is delivered in liposomes (B, column 4). Control experiments using liposomes only (B, column 2) or rebamipide only (B, column 3) show no effect on Zap-70 phosphorylation levels.

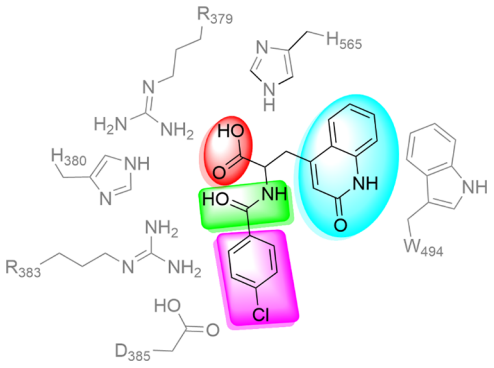

Figure 7. Features of rebamipide that are important contributors to activity. From our SAR and structural studies, rebamipide appears to contain several features that are critical for its ability to inhibit Sts-1. These include the quinolinone (cyan) that makes a π-stacking interaction with W494, the acid (red) that sits in the phosphate binding site, the amide (green), which most likely drives the low energy conformation that is seen in the active site, and the terminal substituted phenyl group (purple). The latter makes a π-cation interaction with R383 but can tolerate a number of different substitutions around the ring.

carboxylic acid, which occupies the phosphate binding site (Figure 7, red); and (4) a backbone amide (Figure 7, green), that likely contributes to stabilize the low energy conformation that the molecule assumes when binding into the Sst-1_{HP} active site. Analysis of the structure around the active site (Figure S9) reveals additional pockets beyond the *p*-phenyl position of rebamipide that may account for the high activity of compound **28**. While rebamipide is poorly cell permeable, when delivered into cells via liposomes, this compound can effectively inhibit PTP activity of Sts-1 and promote Zap-70 phosphorylation. If this liability can be overcome, perhaps through the addition of solubility and/or permeability-enhancing groups or by masking the acid as an ester prodrug, this class of compound could form the basis for a new class of immune-enhancing antibiotics. Our data suggests that substitutions or additions at the phenyl ring are well tolerated and can be employed to generate inhibitors with sub-μM activity.

EXPERIMENTAL SECTION

Protein Expression and Purification. Human Sts-1_{HP} protein was expressed and purified as previously described.[5c] The purified protein was buffer exchanged into storage buffer containing 20 mM HEPES, pH 7.5, 200 mM NaCl, and 5 mM βME, concentrated to 20 mg/mL, aliquoted and flash frozen in liquid nitrogen before being stored at 193 K. Fresh aliquots were thawed on ice before use in kinetics, inhibition, or crystallization experiments. Sts-2_{HP} protein was similarly expressed and purified using established methods.[5c] Sts-2_{HP} was buffer exchanged into the storage buffer, concentrated to 1 mg/mL before being aliquoted and flash frozen. The proteins PTP-1B, SHP1, and CD45 were obtained commercially (AbCam) and were used without further purification.

Sts-1_{HP} Enzyme Assays. Three previously described phosphatase assays[5c] were employed to measure Sts-1_{HP} activity. These assays make use of three different substrates: *p*-nitrophenyl phosphate (pNPP), 3-*O*-methylfluorescein phosphate (OMFP), or 6,8-difluoro-4-methylumbelliferyl phosphate (DifMUP). Briefly, the pNPP assay is run in reaction buffer that contains 20 mM Tris, pH 7.5, 150 mM

https://doi.org/10.1021/acs.jmedchem.3c01763
J. Med. Chem. 2024, 67, 1949−1960

NaCl, 5 mM $MgCl_2$, and 1 mM β-mercaptoethanol. Upon addition of protein, the conversion of pNPP to *p*-nitrophenol is quantified continuously at 298 K by measuring absorbance at 405 nm. For the OMFP substrate, the reaction buffer contains 30 mM Tris, pH 7.4, 75 mM NaCl, 1 mM EDTA, and 1 mM DTT. The reaction progress was monitored continuously by continuous measurement of the fluorescence of the product, 3-*O*-methylfluorescein (λ_{ex} = 485 and λ_{em} = 525 nm). The DifMUP reaction was run in 50 mM Bis-Tris buffer, pH 7.5, 75 mM NaCl, 2 mM EDTA, and 1 mM DTT. In this case, the fluorescence of the 6,8-difluoro-4-methylumbelliferyl product (λ_{ex} = 360, and λ_{em} = 450 nm) was continuously measured at 298 K.

High-Throughput Screen of 590,000 Compounds. The screen was conducted with slight modifications to our previously described approach.[10b] The primary ultrahigh-throughput screening (uHTS) campaign was performed in a 1536-well format, testing one compound per well using a fully automated HTS robotic platform.[11] Two sets of controls, N = 24 per set, were placed on every assay plate: the high control (no enzyme) and the low control (enzyme), both controls containing DMSO (0.58% final). Controls for high inhibition consisted of OMFP substrate and DMSO in the absence of enzyme and the low control consisted of the STS1 protein in the presence of the OMFP substrate and DMSO. These controls were used to ensure STS1 protein activity, to normalize the data and to monitor the data quality by measuring Z' and signal-to-background. All primary HTS data were normalized to the no enzyme control vs protein and were used to produce a scatterplot to aid in visualization of the activity across the HTS campaign.

STS1 protein was prepared in assay buffer (30 mM Tris HCl pH 7.43, 75 mM NaCl, 1 mM EDTA, 1 mM DTT, and 0.001% Tween20) at a final concentration of 750 ng/mL. Prior to the start of the assay, four microliters of assay buffer were dispensed into control wells located in columns 1 through 2 of 1536-well black solid bottom microtiter plates. Next, four microliters of assay buffer containing 1.13 μg/mL of STS1 protein were dispensed into the remaining columns. Then, 35 nL of the test compound in DMSO or DMSO alone (0.58% final concentration) was added to the appropriate wells using the automated GNF/Kalypsys robotic platform. The OMFP substrate was prepared in water as per the original protocol at a final concentration of 50 μM. 1 μL of OMFP solution was added into all wells. Plates were incubated for 20 min at 25 °C. To stop the reaction, 1 μL of NaOH was dispensed into all the wells using the dispenser described above. Then, after 20 min of incubation at 25 °C, fluorescence was measured at 485 nm excitation and 535 nm emission using a ViewLux plate reader (PerkinElmer, Waltham, MA). The counterscreen assay that was utilized used the same reagents as the primary assay but the compounds were added after the NaOH step to help identify fluorescent quenchers and other nonspecific inhibitors. Compounds that are active in both assays are considered as possible quenchers or potential artifacts of the assay.

Screening Library. The UF Scripps Drug Discovery Library (SDDL) has been described elsewhere and was commercially acquired from commercial vendor resources around the world.[17] By design, the diversity of the SDDL mimics that of much larger collections found at major pharmaceutical companies yet is responsive to lessons learned from successful drug discovery efforts and emerging trends in HTS library construction.

Screening Data. Raw fluorescent data were uploaded into the UF Scripps Research Institutes Molecular Screening Center (SRIMSC) HTS database (Symyx, Santa Clara, CA). Activity of each well was normalized on a per-plate basis using the following equation:

$$\%\text{Inhibition} = 100 \times \frac{\text{Test well} - \text{Median Low Control}}{\text{Median High Control} - \text{Median Low Control}}$$

where the low control is defined as wells containing the STS1 protein in the presence of DMSO and the OMFP substrate. The test well is defined as the median of the wells containing test compounds, and high control is defined as the wells containing DMSO and OMFP but no STS1 protein. The Z' and S:B for this assay is calculated using the high control and low control wells. PHPS1, a known STS-1 inhibitor, was used as a reference control. PHPS1 yielded ~70% max inhibition, so it was only used as a reference and not as a high control. Data were normalized on a per plate basis, and each assay plate underwent a quality control check. A value greater than 0.5 for Z' was required before further testing.[18] For the primary screen, test compounds from the library were screened in singlicate at a final nominal concentration of 5.8 μM (final DMSO concentration of 0.58%). Well fluorescence was measured with a ViewLux plate reader (PerkinElmer, Waltham, MA), and the percent inhibition of each test compound was calculated on a per-plate basis. A mathematical algorithm was used to determine nominally inhibiting compounds in the primary screen. Four values were calculated to determine an interval-based cutoff: (1) the average percent inhibition of all high controls tested plus three times the standard deviation of the high controls, (2) the average percent inhibition of all low controls tested minus three times the standard deviation of the low controls, (3) the average percent inhibition of all compounds tested between (1) and (2), and (4) three times their standard deviation. The sum of two of these values, (3) and (4), was used as a cutoff parameter. Any compound that exhibited greater % inhibition than the cutoff parameter was declared active.

Dose Response Assays. For dose−response experiments, the average of triplicate well data was plotted against compound concentration. A four-parameter equation describing a sigmoidal dose−response curve was fitted using assay explorer software (Symyx-MDL Information Systems).

HTS Confirmation and Tertiary Assays. The confirmation screen was run under the same conditions as the primary HTS except that plates were assessed in triplicate and results for each compound were reported as the average percentage inhibition of the three measurements, plus or minus the associated standard deviation. For titration experiments, assay protocols were identical to those described above, with the following exception that compounds were prepared in 10 point, 1:3 serial dilutions starting at a nominal test concentration of 14.5 μM, and assessed in triplicate.

Measurement of IC_{50} and K_i of Inhibitors. All measurements of IC_{50} and K_i were conducted in 96-well microplates (UV Star, Thermo) with a total volume of 200 μL. To ensure consistency and reproducibility in our measurements, we used a spectrophotometer equipped with an autoinjector (Synergy Neo2, BioTek). An 8-point 2-fold serial dilution of the compound was generated in triplicate from a 10 mM stock in DMSO. The Sts-1_{HP} enzyme (1.5 μg/mL) or other PTP (CD45, 1.5 μg/mL; PTP-1B, 10 μg/mL; SHP-2, 3.5 μg/mL) was incubated with the inhibitor for 20 min prior to addition of the substrate (DiFMUP, 1.5 μM; pNPP, 1 mM; OMFP, 150 μM) by autoinjection to initiate the reaction. The initial rates of reaction were compared to a vehicle control reaction to determine percent activity at each inhibitor concentration. The percent activity was plotted against the concentration of inhibitor used on a log scale and was fit with a 4-parameter logistic equation. The reported IC_{50} values are the value of the X-intercept at 50% activity level. The inhibition constant, K_i, of rebamipide was calculated by measuring the initial rates of Sts-1_{HP} activity, over a range of DiFMUP concentrations (1−1000 μM), in the presence of 0, 10, 50, or 100 μM rebamipide. Initial velocities were calculated from progress curves before the reactions had reached 10% completion, and the initial rates were plotted against substrate concentration. Each data set was an individual fit with the Michaelis−Menten eq 1, and the K_i value was determined from the apparent K_M using eq 2.

$$v_O = \frac{V_{max}[S]}{K_{M(app)} + [S]} \quad (1)$$

where v_O is the initial velocity, V_{max} is the maximum velocity, S is the substrate concentration, and $K_{M(app)}$ is the calculated K_M (substrate concentration at half the maximum rate).

$$K_{M(app)} = K_M\left(1 + \frac{[i]}{K_i}\right) \quad (2)$$

https://doi.org/10.1021/acs.jmedchem.3c01763
J. Med. Chem. 2024, 67, 1949−1960

where K_M is the known Michaelis−Menten constant (substrate concentration at half the maximum rate) for the substrate (DiFMUP, 2 μM),[5c] [i] is the inhibitor concentration, and K_i is the inhibition constant.

Cell-Based Assays of Sts-1 Activity. To determine if rebamipide, or rebamipide in liposomes, could enter the cell and inhibit Sts-1, we used a previously described Zap-70 dephosphorylation assay[5a,c] as well as assaying Zap-70 dephosphorylation in Jurkat. For the former, human embryonic kidney 293 cells (ATTC) were cultured in DMEM (Gibco) supplemented with 10% FBS (Fisher Hyclone) and 100 units/mL of penicillin and 100 units/mL of streptomycin. Flag-tagged Sts-1 was cotransfected into cells using Lipofectamine 2000 (Invitrogen) along with plasmids encoding lymphocyte-specific protein tyrosine kinase, T7-tagged Zap-70, and a CD8-ζ chain chimera. Twenty four hours after transfection, the cells were lysed in buffer containing 50 mM Tris, pH 7.6, 150 mM NaCl, 5 mM EDTA, and 1% NP-50 and clarified by centrifugation for 15 min at 16,000g. Lystates were suspended in Laemmli sample buffer, and proteins were resolved by SDS-PAGE and then transferred to a nitrocellulose membrane for immunoblotting. Phosphorylation of Zap-70 was determined by comparing the quantity of phospho-Zap-70 with a pTyr-493 specific antibody (Cell Signaling Technologies) to the levels of total Zap-70 using a T7 specific antibody (Novagen). The effect of rebamipide on Sts-1 dephosphorylation of Zap-70 was determined by incubating the cells in various concentrations (50, 75, 100, or 200 μM) of rebamipide for 20 min prior to analysis. To assess the role of cell permeability in rebamipide-mediated inhibition of Sts-1, we used lipofection (Lipofectamine 2000, Thermo) to aid in the cell entry of rebamipide and compared Zap-70 phosphorylation in these samples to controls without liposomes or using empty liposomes. For Jurkat cells (ATCC), cells were cultured in RMPI 1640 (Gibco) supplemented with 10% FBS (Fisher Hyclone), 100 units/mL of penicillin, and 100 units/mL of streptomycin. Treatment with rebamipide, lipofectamine, and rebamipide with lipofectamine was carried out as described above. Phospho-Zap-70 was detected as described above while total Zap-70 and Sts-1 were detected using Zap-70 and Sts-specific antibodies (Cell Signaling Technologies and ProteinTech, respectively). Note that, due to the similar molecular weights of Zap-70 and Sts, identical samples were run in parallel and separately blotted for either Zap-70 or Sts-1. In both cases, GAPDH was used as a loading control (see Figure 6B).

Crystallization, Structure Determination, and Refinement. Protein crystals of rebamipide-Sts-1_{HP} were obtained using hanging drop vapor diffusion with an equal volume of 20 mg/mL Sts-1_{HP} containing 10 mM rebamipide and well solution in a 3 μL drop over 350 μL of well solution containing 0.1 M Hepes (pH 7.0), 10% ethylene glycol, 0.3 M magnesium chloride, and 20% PEG 8000. Crystals appeared after 3−6 days incubation at 291 K. Prior to freezing by plunging in liquid nitrogen, crystals were transferred to a solution containing well solution supplemented with 5 mM rebamipide and 20% ethylene glycol. Diffraction data were collected at 100 K at the Northeast Collaborative Access Team 24-ID-E beamline of the Advanced Photon Source at Argonne National Lab. Data were indexed, integrated, and scaled using the modular RAPD suite implemented at NE-CAT that uses Labelit for indexing, XDS to integrate and scale the data, and Pointless and Scala for additional analysis and merging.[19] Phases were determined by molecular replacement using Molrep in the CCP4 suite of programs with a protomer of the solved structure of Sts-1_{HP} as a search model (PDB identifier 5VR6).[5c,20] The final structure was built through iterative rounds of manual model building using Coot and refinement using REFMAC5.[21] Waters were added manually after the refinement had converged. The rebamipide structure was built into difference density of the fully refined structure and then subjected to an additional round of refinement. Restraints for rebamipide and for compound **11** were generated using eLBOW in the PHENIX suite of programs.[22] Data collection and refinement statistics are included in Table S2.

Synthesis of Rebamipide Analogs. All chemicals and reagents were purchased from Sigma-Aldrich, Fisher Scientific, Oakwood Chemicals, Combi-blocks,or Ambeed and were used without further purification unless otherwise specified. Reported compounds are >95% pure by HPLC analysis. Analytical TLC of all reactions was performed on Sigma-Aldrich prepared plates (silica gel 60 F-254 on glass). ^{1}H and ^{13}C NMRs were recorded on a Bruker 500 MHz spectrometer (Avance) in DMSO-d_6 with TMS (0 ppm) as an internal standard, and the data were processed using Mnova software (Mestrelab Research). Coupling constants are reported in Hertz (Hz). ESI mass spectra were recorded on an AB Sciex TripleTof 5600 mass spectrometer. Yields were not optimized. Example HPLC traces of rebamipide (1), compound 11, and compound 28 are provided in Figure S10.

*Synthesis of (4-Chlorobenzoyl)-L-tryptophan (200), (4-Chlorobenzoyl)-D-tryptophan (**2**).* To a stirred solution of L-tryptophan (204 mg, 1 mmol) and sodium hydroxide (120 mg, 3 mmol) in water (2.0 mL) at 0 °C was added a solution of 4-chlrobenzoyl chloride (175 mg, 1 mmol) in acetone (2.0 mL). The resulting mixture was stirred at room temperature for 2 h. After this time, the reaction mixture was diluted with water and acidified with 2 N HCl. The formed precipitate was filtered, washed with water, and purified by recrystallization. ^{1}H NMR (500 MHz, DMSO-d_6) δ 12.76 (bs, 1H), 10.80 (s, 1H), 8.75 (d, J = 7.8 Hz, 1H), 7.84 (d, J = 8.4 Hz, 2H), 7.59 (d, J = 7.9 Hz, 1H), 7.55−7.50 (m, 2H), 7.32 (d, J = 8.0 Hz, 1H), 7.19 (d, J = 2.4 Hz, 1H), 7.05 (t, J = 7.5 Hz, 1H), 6.98 (t, J = 7.4 Hz, 1H), 4.61−4.68 (m, 1H), 3.31 (dd, J = 14.6, 4.6 Hz, 1H), 3.20 (dd, J = 14.6, 10.0 Hz, 1H). ^{13}C NMR (126 MHz, DMSO-d_6) δ 173.34, 165.17, 136.05, 135.98, 132.56, 129.20, 128.22, 127.01, 123.41, 120.82, 118.26, 118.00, 111.31, 110.28, 53.68, 26.52. MS (ESI−): 341.3 [M − 1].

*Synthesis of 2-(4-Chlorobenzamido)-3-(3,4-dihydronaphthalen-1-yl)propanoic Acid (**3**).* To a stirred solution of 2-amino-3-(naphthalen-1-yl) propanoic acid hydrochloride (251.7 mg, 1 mmol) and sodium hydroxide (120 mg, 3 mmol) in water (2.5 mL) at 0 °C was added a solution of substituted 4-chlorobenzoyl chloride (175 mg, 1 mmol) in acetone (2.5 mL). The resulting mixture was stirred at room temperature overnight. Subsequently, the reaction mixture was diluted with water and acidified with 2 N HCl. The solution was extracted with ethyl acetate, washed with water and brine, and dried over sodium sulfate. The ethyl acetate layer was evaporated, and the obtained residue was purified by column chromatography using ethyl acetate and hexane. ^{1}H NMR (301 MHz, DMSO) δ 8.89 (d, J = 8.1 Hz, 1H), 8.20 (d, J = 8.4 Hz, 1H), 7.94 (dd, J = 8.3, 3.5 Hz, 1H), 7.75−7.82 (m, 3H), 7.67−7.46 (m, 5H), 7.40 (t, J = 7.6 Hz, 1H), 4.81−4.67 (m, 1H), 3.77 (dd, J = 14.1, 4.0 Hz, 1H), 3.55−3.41 (m, 1H). MS (ESI−): 354.2 [M − 1].

General Procedure for the Synthesis of 2-Amino-3-(2-oxo-1,2-dihydroquinolin-4-yl) Propanoic acid Derivatives. To a stirred solution of 2-amino-3-(2-oxo-1,2-dihydroquinolin-4-yl)propanoic acid hydrochloride (269 mg, 1 mmol) and sodium hydroxide (120 mg, 3 mmol) in water (2.5 mL) at 0 °C was added a solution of substituted benzoyl chloride (1 mmol) in acetone (2.5 mL). The resulting mixture was stirred at room temperature overnight. Subsequently, the reaction mixture was diluted with water and acidified with 2 N HCl. The formed precipitate was filtered and washed with water and ethyl acetate. The product was then purified by recrystallization using an appropriate solvent system (DMF, DMF-water, ethanol, or ethanol−water).

*Synthesis of 2-(2-Naphthamido)-3-(2-oxo-1,2-dihydroquinolin-4-yl)propanoic Acid (**4**).* The compound **4** was prepared by using 2-amino-3-(2-oxo-1,2-dihydroquinolin-4-yl)propanoic acid hydrochloride, NaOH, and 2-naphthoyl chloride as described in the above general procedure. ^{1}H NMR (500 MHz, DMSO-d_6) δ 13.08 (s, 1H), 11.65 (s, 1H), 8.97 (d, J = 7.9 Hz, 1H), 8.41 (d, J = 1.7 Hz, 1H), 8.05−7.93 (m, 3H), 7.92−7.84 (m, 2H), 7.57−7.65 (m, 2H), 7.51 (t, J = 7.7 Hz, 1H), 7.32 (d, J = 8.2 Hz, 1H), 7.29−7.21 (m, 1H), 6.51 (s, 1H), 4.78−4.86 (m, 1H), 3.69−3.40 (m, 1H), 3.20−3.31 (m, 1H). MS (ESI−): 385.3 [M − 1].

*Synthesis of 3-(2-Oxo-1,2-dihydroquinolin-4-yl)-2-(thiophene-2-carboxamido)propanoic Acid (**5**).* The compound **5** was prepared by using 2-amino-3-(2-oxo-1,2-dihydroquinolin-4-yl)propanoic acid hydrochloride, NaOH, and 2-thiophenecarbonyl chloride as described in

https://doi.org/10.1021/acs.jmedchem.3c01763
J. Med. Chem. 2024, 67, 1949−1960

the above general procedure. ^{1}H NMR (500 MHz, DMSO-d_6) δ 13.06 (s, 1H), 11.65 (s, 1H), 8.84 (d, J = 8.3 Hz, 1H), 7.87−7.74 (m, 3H), 7.48−7.53 (m, 1H), 7.32 (d, J = 8.4 Hz, 1H), 7.21−7.26 (m, 1H), 7.15 (dd, J = 5.0, 3.7 Hz, 1H), 6.45 (s, 1H), 4.67−4.74 (m, 1H), 3.48 (dd, J = 14.4, 4.0 Hz, 1H), 3.21 (dd, J = 14.4, 10.7 Hz, 1H). MS (ESI−): 341.3 [M − 1].

*Synthesis of 2-(6-Chloronicotinamido)-3-(2-oxo-1,2-dihydroquinolin-4-yl)propanoic Acid (**6**).* The compound **6** was prepared by using 2-amino-3-(2-oxo-1,2-dihydroquinolin-4-yl)propanoic acid hydrochloride, NaOH, and 6-chloronicotinoyl chloride as described in the above general procedure. ^{1}H NMR (500 MHz, DMSO-d_6) δ 13.13 (s, 1H), 11.66 (s, 1H), 9.14 (d, J = 8.1 Hz, 1H), 8.77 (d, J = 2.4 Hz, 1H), 8.19 (dd, J = 8.3, 2.5 Hz, 1H), 7.84 (d, J = 8.0 Hz, 1H), 7.66 (d, J = 8.3 Hz, 1H), 7.57−7.45 (m, 1H), 7.32 (d, J = 8.1 Hz, 1H), 7.23 (t, J = 7.6 Hz, 1H), 6.45 (s, 1H), 4.79−4.73 (m, 1H), 3.50 (dd, J = 14.3, 4.1 Hz, 1H), 3.23 (dd, J = 14.4, 10.5 Hz, 1H). ^{13}C NMR (126 MHz, DMSO-d_6) δ 172.30, 163.92, 161.27, 152.86, 148.95, 147.16, 138.96, 138.61, 130.33, 128.56, 124.23, 124.00, 121.89, 121.80, 118.49, 115.84, 51.96, 32.86. MS (ESI−): 370.3 [M − 1].

*Synthesis of 2-(4-Fluorobenzamido)-3-(2-oxo-1,2-dihydroquinolin-4-yl)propanoic Acid (**7**).* The compound **7** was prepared by using 2-amino-3-(2-oxo-1,2-dihydroquinolin-4-yl)propanoic acid hydrochloride, NaOH, and 4-fluorobenzoyl chloride as described in the above general procedure. ^{1}H NMR (500 MHz, DMSO-d_6) δ 13.03 (bs, 1H), 11.65 (s, 1H), 8.85 (d, J = 8.2 Hz, 1H), 7.92−7.80 (m, 3H), 7.49−7.53 (m, 1H), 7.28−7.33 (m, 3H), 7.24 (t, J = 7.1 Hz, 1H), 6.46 (s, 1H), 4.88−4.59 (m, 1H), 3.49 (dd, J = 14.3, 3.9 Hz, 1H), 3.24 (dd, J = 14.4, 10.7 Hz, 1H). MS (ESI+): 355.2 [M + 1]

*Synthesis of 2-(4-Methylbenzamido)-3-(2-oxo-1,2-dihydroquinolin-4-yl)propanoic Acid (**8**).* The compound **8** was prepared by using 2-amino-3-(2-oxo-1,2-dihydroquinolin-4-yl)propanoic acid hydrochloride, NaOH, and 4-methylbenzoyl chloride as described in the above general procedure. ^{1}H NMR (500 MHz, DMSO-d_6) δ 12.98 (s, 1H), 11.64 (s, 1H), 8.71 (d, J = 8.2 Hz, 1H), 7.84 (dd, J = 8.2, 1.3 Hz, 1H), 7.71 (d, J = 8.2 Hz, 2H), 7.47−7.53 (m, 1H), 7.31 (d, J = 8.3 Hz, 1H), 7.28−7.21 (m, 3H), 6.46 (s, 1H), 4.84−4.65 (m, 1H), 3.48 (dd, J = 14.3, 3.9 Hz, 1H), 3.24 (dd, J = 14.4, 10.8 Hz, 1H), 2.34 (s, 3H). ^{13}C NMR (126 MHz, DMSO-d_6) δ 172.74, 166.17, 161.21, 147.31, 141.32, 138.85, 130.78, 130.17, 128.71, 127.23, 123.91, 121.78, 121.63, 118.44, 115.72, 51.66, 32.77, 20.86. MS (ESI+): 351.2 [M + 1].

*Synthesis of 2-((4-Methylphenyl)sulfonamido)-3-(2-oxo-1,2-dihydroquinolin-4-yl)propanoic Acid (**23**).* The compound **23** was prepared by using 2-amino-3-(2-oxo-1,2-dihydroquinolin-4-yl)-propanoic acid hydrochloride, NaOH, and p-toluenesulfonyl chloride as described in the above general procedure. ^{1}H NMR (500 MHz, DMSO-d_6) δ 13.04 (s, 1H), 11.52 (s, 1H), 8.37 (d, J = 8.8 Hz, 1H), 7.45 (dd, J = 8.0, 6.5 Hz, 2H), 7.30 (d, J = 8.4 Hz, 2H), 7.26−7.21 (m, 1H), 7.19−7.09 (m, 1H), 7.02 (d, J = 8.0 Hz, 2H), 6.33 (s, 1H), 3.23 (dd, J = 13.9, 4.4 Hz, 1H), 2.77 (dd, J = 13.9, 10.1 Hz, 1H), 2.29 (s, 3H). ^{13}C NMR (126 MHz, DMSO-d_6) δ 172.10, 161.01, 145.32, 142.15, 138.81, 137.36, 129.90, 128.87, 125.74, 123.35, 122.91, 121.53, 117.83, 115.62, 54.78, 34.30, 20.88. MS (ESI+): 387.2 [M + 1].

*Synthesis of 3-(2-Oxo-1,2-dihydroquinolin-4-yl)-2-(4-(trifluoromethyl)benzamido)propanoic Acid (**9**).* The compound **9** was prepared by using 2-amino-3-(2-oxo-1,2-dihydroquinolin-4-yl)-propanoic acid hydrochloride, NaOH, and 4-trifluoromethylbenzoyl chloride as described in the above general procedure. ^{1}H NMR (500 MHz, DMSO-d_6) δ 11.58 (s, 1H), 8.64 (d, J = 8.0 Hz, 1H), 7.99−7.91 (m, 3H), 7.81 (d, J = 8.1 Hz, 2H), 7.44−7.50 (m, 1H), 7.32 (d, J = 8.3, 1H), 7.17−7.23 (m, 1H), 6.42 (s, 1H), 4.56 (m, 1H), 3.53 (dd, J = 14.0, 3.8 Hz, 1H), 3.11 (dd, J = 14.0, 9.8 Hz, 1H). MS (ESI+): 405.2 [M + 1].

*Synthesis of 2-(4-Cyanobenzamido)-3-(2-oxo-1,2-dihydroquinolin-4-yl)propanoic Acid (**10**).* The compound **10** was prepared by using 2-amino-3-(2-oxo-1,2-dihydroquinolin-4-yl)propanoic acid hydrochloride, NaOH, and 4-cyanobenzoyl chloride as described in the above general procedure. ^{1}H NMR (500 MHz, DMSO-d_6) δ 13.13 (s, 1H), 11.65 (s, 1H), 9.09 (d, J = 8.2 Hz, 1H), 8.00−7.90 (m, 5H), 7.84 (d, J = 8.0 Hz, 1H), 7.54−7.47 (m, 1H), 7.31 (d, J = 8.2 Hz, 1H), 7.21−7.26 (m, 1H), 6.45 (s, 1H), 4.79−4.71 (m, 1H), 3.51 (dd, J = 14.3, 3.9 Hz, 1H), 3.23 (dd, J = 14.4, 10.7 Hz, 1H). ^{13}C NMR (126 MHz, DMSO-d_6) δ 172.32, 164.95, 161.18, 147.18, 138.86, 137.49, 132.40, 130.21, 128.01, 123.90, 121.80, 121.61, 118.40, 118.16, 115.74, 113.79, 51.96, 32.75. MS (ESI+): 362.2 [M + 1].

*Synthesis of 2-(4-Ethylbenzamido)-3-(2-oxo-1,2-dihydroquinolin-4-yl)propanoic Acid (**11**).* The compound **11** was prepared by using 2-amino-3-(2-oxo-1,2-dihydroquinolin-4-yl)propanoic acid hydrochloride, NaOH, and 4-ethylbenzoyl chloride as described in the above general procedure. ^{1}H NMR (500 MHz, DMSO-d_6) δ 12.97 (s, 1H), 11.64 (s, 1H), 8.72 (d, J = 8.2 Hz, 1H), 7.85 (d, J = 8.0 Hz, 1H), 7.74 (d, J = 8.4 Hz, 1H), 7.48−7.53 (m, 1H), 7.36−7.21 (m, 4H), 6.46 (s, 1H), 4.71−4.78 (m, 1H), 3.49 (dd, J = 14.3, 3.8 Hz, 1H), 3.24 (dd, J = 14.4, 10.8 Hz, 1H), 2.64 (q, J = 7.6 Hz, 2H), 1.18 (t, J = 7.6 Hz, 3H). ^{13}C NMR (126 MHz, DMSO-d_6) δ 172.75, 166.20, 161.21, 147.50, 147.31, 138.86, 131.07, 130.18, 127.55, 127.32, 123.91, 121.79, 121.64, 118.44, 115.73, 51.64, 32.78, 27.92, 15.23. MS (ESI+): 365.2 [M + 1].

*Synthesis of 3-(2-Oxo-1,2-dihydroquinolin-4-yl)-2-(4-(trifluoromethoxy)benzamido)propanoic Acid (**12**).* The compound **12** was prepared by using 2-amino-3-(2-oxo-1,2-dihydroquinolin-4-yl)propanoic acid hydrochloride, NaOH, and 4-trifluoromethoxybenzoyl chloride as described in the above general procedure. ^{1}H NMR (500 MHz, DMSO-d_6) δ 13.06 (s, 1H), 11.65 (s, 1H), 8.95 (d, J = 8.2 Hz, 1H), 7.93 (d, J = 8.8 Hz, 2H), 7.84 (d, J = 8.1, 1H), 7.53−7.42 (m, 3H), 7.32 (d, J = 8.2, 1H), 7.22−7.26 (m, 1H), 6.45 (s, 1H), 4.79−4.69 (m, 1H), 3.50 (dd, J = 14.4, 3.9 Hz, 1H), 3.24 (dd, J = 14.4, 10.7 Hz, 1H). ^{13}C NMR (126 MHz, DMSO-d_6) δ 172.50, 165.13, 161.20, 150.36, 147.21, 138.87, 132.64, 130.21, 129.56, 123.90, 121.81, 121.61, 120.58, 118.42, 115.75, 51.82, 32.75. MS (ESI+): 421.2 [M + 1].

*Synthesis of 2-(4-Methoxybenzamido)-3-(2-oxo-1,2-dihydroquinolin-4-yl)propanoic Acid (**13**).* The compound **13** was prepared by using 2-amino-3-(2-oxo-1,2-dihydroquinolin-4-yl)propanoic acid hydrochloride, NaOH, and 4-methoxybenzoyl chloride as described in the above general procedure. ^{1}H NMR (500 MHz, DMSO-d_6) δ 12.90 (s, 1H), 11.64 (s, 1H), 8.65 (d, J = 8.2 Hz, 1H), 7.93−7.75 (m, 3H), 7.51 (m, 1H), 7.32 (d, J = 8.2 1H), 7.21−7.27 (m, 1H), 7.05−6.95 (m, 2H), 6.46 (s, 1H), 4.77−4.69 (m, 1H), 3.80 (s, 2H), 3.48 (dd, J = 14.3, 3.8 Hz, 1H), 3.24 (dd, J = 14.4, 10.8 Hz, 1H). ^{13}C NMR (126 MHz, DMSO-d_6) δ 172.84, 165.78, 161.67, 161.21, 147.33, 138.85, 131.23, 130.17, 129.09, 125.75, 123.90, 121.78, 121.64, 118.43, 115.73, 113.70, 113.41, 55.25, 51.65, 32.79. MS (ESI−): 365.3 [M − 1].

*Synthesis of 2-(2-Chlorobenzamido)-3-(2-oxo-1,2-dihydroquinolin-4-yl)propanoic Acid (**16**).* The compound **16** was prepared by using 2-amino-3-(2-oxo-1,2-dihydroquinolin-4-yl)propanoic acid hydrochloride, NaOH, and 2-chlorobenzoyl chloride as described in the above general procedure. ^{1}H NMR (500 MHz, DMSO-d_6) δ 13.08 (s, 1H), 11.66 (s, 1H), 8.88 (d, J = 8.3 Hz, 1H), 7.83 (dd, J = 8.2, 1.4 Hz, 1H), 7.57−7.20 (m, 7H), 6.48 (s, 1H), 4.72 (m, 1H), 3.48 (dd, J = 14.4, 3.8 Hz, 1H), 3.10 (dd, J = 14.5, 10.8 Hz, 1H). ^{13}C NMR (126 MHz, DMSO-d_6) δ 172.24, 166.19, 161.22, 146.71, 138.91, 136.11, 130.86, 130.15, 129.86, 129.56, 128.68, 126.87, 123.88, 122.05, 121.79, 118.42, 115.72, 51.37, 32.89. MS (ESI+): 371.2 [M + 1].

*Synthesis of 2-(3,4-Dichlorobenzamido)-3-(2-oxo-1,2-dihydroquinolin-4-yl)propanoic Acid (**17**).* The compound **17** was prepared by using 2-amino-3-(2-oxo-1,2-dihydroquinolin-4-yl)propanoic acid hydrochloride, NaOH, and 3,4-dichlorobenzoyl chloride as described in the above general procedure. ^{1}H NMR (500 MHz, DMSO-d_6) δ 11.59 (s, 1H), 8.75 (d, J = 8.2 Hz, 1H), 8.01 (d, J = 2.0 Hz, 1H), 7.90 (d, J = 8.1 Hz, 1H), 7.79−7.69 (m, 2H), 7.45−7.50 (m, 1H), 7.30 (d, J = 8.1 Hz, 1H), 7.24−7.17 (m, 1H), 6.41 (s, 1H), 4.56−4.64 (m, 1H), 3.52 (dd, J = 14.1, 3.7 Hz, 1H), 3.12 (dd, J = 14.2, 10.2 Hz, 1H). MS (ESI−): 403.3 [M − 1].

*Synthesis of 2-(3-Chlorobenzamido)-3-(2-oxo-1,2-dihydroquinolin-4-yl)propanoic Acid (**18**).* The compound **18** was prepared by using 2-amino-3-(2-oxo-1,2-dihydroquinolin-4-yl)propanoic acid hydrochloride, NaOH, and 3-chlorobenzoyl chloride as described in the

https://doi.org/10.1021/acs.jmedchem.3c01763
J. Med. Chem. 2024, 67, 1949−1960

above general procedure. ^{1}H NMR (500 MHz, DMSO-d_6) δ 11.65 (s, 1H), 8.93 (d, J = 8.2 Hz, 1H), 7.89−7.80 (m, 2H), 7.76 (dt, J = 7.8, 1.4 Hz, 1H), 7.62 (dq, J = 8.0, 2.2 Hz, 1H), 7.51 (td, J = 7.6, 1.3 Hz, 2H), 7.32 (d, J = 8.3, Hz, 1H), 7.21−7.26 (m, 1H), 6.45 (s, 1H), 4.81−4.58 (m, 1H), 3.50 (dd, J = 14.4, 3.9 Hz, 1H), 3.23 (dd, J = 14.5, 10.7 Hz, 1H). ^{13}C NMR (126 MHz, DMSO-d_6) δ 172.49, 164.86, 161.21, 147.30, 138.86, 135.57, 133.09, 131.26, 130.30, 130.19, 126.95, 125.99, 123.94, 121.78, 121.56, 118.46, 115.73, 51.96, 32.81. MS (ESI−): 369.3 [M − 1].

*Synthesis of 3-(2-Oxo-1,2-dihydroquinolin-4-yl)-2-(3-(trifluoromethyl)benzamido)propanoic Acid (**19**).* The compound **19** was prepared by using 2-amino-3-(2-oxo-1,2-dihydroquinolin-4-yl)propanoic acid hydrochloride, NaOH, and 3-trifluorobenzoyl chloride as described in the above general procedure. H NMR (500 MHz, DMSO-d_6) δ 11.64 (s, 1H), 9.07 (d, J = 8.2 Hz, 1H), 8.18−8.05 (m, 2H), 7.92 (d, J = 7.8 Hz, 1H), 7.87 (d, J = 8.2 Hz, 1H), 7.47−7.53 (m, 1H), 7.31 (d, J = 8.4 Hz, 1H), 7.20−7.25 (m, 1H), 6.45 (s, 1H), 4.74−4.80 (m, 1H), 3.51 (dd, J = 14.3, 4.0 Hz, 1H), 3.24 (dd, J = 14.4, 10.5 Hz, 1H). MS (ESI+): 405.2 [M + 1].

*Synthesis of 2-(3,4-Difluorobenzamido)-3-(2-oxo-1,2-dihydroquinolin-4-yl)propanoic Acid (**20**).* The compound **20** was prepared by using 2-amino-3-(2-oxo-1,2-dihydroquinolin-4-yl)propanoic acid hydrochloride, NaOH, and 3,4-difluorobenzoyl chloride as described in the above general procedure. ^{1}H NMR (500 MHz, DMSO-d_6) δ 11.65 (s, 1H), 8.91 (d, J = 8.2 Hz, 1H), 7.88−7.81 (m, 2H), 7.75−7.68 (m, 1H), 7.61−7.47 (m, 2H), 7.31 (d, J = 8.3 Hz, 1H), 7.20−7.26 (m, 1H), 6.44 (s, 1H), 4.79−4.63 (m, 1H), 3.50 (dd, J = 14.3, 3.9 Hz, 1H), 3.21 (dd, J = 14.4, 10.6 Hz, 1H). MS (ESI−): 371.3 [M − 1].

*Synthesis of 2-Acetamido-3-(2-oxo-1,2-dihydroquinolin-4-yl)-propanoic Acid (**26**).* The compound **26** was prepared by using 2-amino-3-(2-oxo-1,2-dihydroquinolin-4-yl)propanoic acid hydrochloride (1 mmol), NaOH (4 mmol), and acetyl chloride (3.0 mmol) as described in the above general procedure. ^{1}H NMR (500 MHz, DMSO-d_6) δ 12.91 (s, 1H), 11.67 (s, 1H), 8.32 (d, J = 8.2 Hz, 1H), 7.79 (d, J = 8.0 Hz, 1H), 7.48−7.53 (m, 1H), 7.32 (d, J = 8.1 Hz 1H), 7.20−7.25 (m, 1H), 6.39 (s, 1H), 4.48−4.54 (m, 1H), 3.39−3.23 (m, 1H), 3.00 (dd, J = 14.3, 9.8 Hz, 1H), 1.79 (s, 3H). ^{13}C NMR (126 MHz, DMSO-d_6) δ 172.66, 169.28, 161.22, 146.92, 138.84, 130.18, 123.91, 121.74, 121.66, 118.42, 115.69, 51.28, 33.35, 22.20. MS (ESI−): 273.2 [M − 1].

*Synthesis of 2-(2-(4-Chlorophenoxy)acetamido)-3-(2-oxo-1,2-dihydroquinolin-4-yl)propanoic Acid (**27**).* The compound **27** was prepared by using 2-amino-3-(2-oxo-1,2-dihydroquinolin-4-yl)-propanoic acid hydrochloride, NaOH, and 2- 2-(4-chlorophenoxy)-acetyl chloride as described in the above general procedure. ^{1}H NMR (500 MHz, DMSO-d_6) δ 11.70 (s, 1H), 8.55 (d, J = 8.4 Hz, 1H), 7.79 (d, J = 8.0 Hz, 1H), 7.47−7.53 (m, 1H), 7.38−7.26 (m, 3H), 7.24−7.19 (m, 1H), 6.91−6.84 (m, 2H), 6.43 (s, 1H), 4.60−4.66 (m, 1H), 4.47 (s, 2H), 3.43 (dd, J = 14.2, 4.1 Hz, 1H), 3.14 (dd, J = 14.3, 10.3 Hz, 1H). MS (ESI−): 399.3 [M − 1].

*Synthesis of 2-(2-(1H-Indol-3-yl)-2-oxoacetamido)-3-(2-oxo-1,2-dihydroquinolin-4-yl)propanoic Acid (**31**).* The compound **31** was prepared by using 2-amino-3-(2-oxo-1,2-dihydroquinolin-4-yl)-propanoic acid hydrochloride, NaOH, and 3-indoleglyoxylyl chloride as described in the above general procedure. ^{1}H NMR (500 MHz, DMSO-d_6) δ 13.15 (s, 1H), 12.25 (d, J = 3.3 Hz, 1H), 11.66 (s, 1H), 9.09 (d, J = 8.4 Hz, 1H), 8.58 (d, J = 3.3 Hz, 1H), 8.24−8.13 (m, 1H), 7.84 (d, J = 8.1 Hz, 1H), 7.57−7.47 (m, 2H), 7.33 (dd, J = 8.3, 1.2 Hz, 1H), 7.36−7.14 (m, 3H), 6.46 (s, 1H), 4.66−4.73 (m, 1H), 3.50 (dd, J = 14.4, 3.9 Hz, 1H), 3.33−3.27 (m, 1H). ^{13}C NMR (126 MHz, DMSO-d_6) δ 181.20, 171.96, 163.56, 161.20, 147.08, 138.86, 138.28, 136.18, 130.19, 125.93, 123.93, 123.41, 122.53, 121.78, 121.63, 121.11, 118.45, 115.72, 112.48, 111.98, 51.16, 32.43. MS (ESI−): 402.3 [M − 1].

*Synthesis of 2-(4-Chloro-3-nitrobenzamido)-3-(2-oxo-1,2-dihydroquinolin-4-yl)propanoic Acid (**21**).* The compound **21** was prepared by using 2-amino-3-(2-oxo-1,2-dihydroquinolin-4-yl)-propanoic acid hydrochloride, NaOH, and 4-chloro-3-nitrobenzoyl chloride as described in the above general procedure. ^{1}H NMR (500 MHz, DMSO-d_6) δ 13.19 (s, 1H), 11.66 (s, 1H), 9.21 (d, J = 8.1 Hz, 1H), 8.47 (d, J = 2.1 Hz, 1H), 8.11 (dd, J = 8.4, 2.1 Hz, 1H), 7.92 (d, J = 8.4 Hz, 1H), 7.85 (d, J = 8.0 Hz, 1H), 7.53−7.48 (m, 1H), 7.31 (d, J = 8.1 Hz, 1H), 7.25−7.20 (m, 1H), 6.43 (s, 1H), 4.81−4.74 (m, 1H), 3.50 (dd, J = 14.4, 4.2 Hz, 1H), 3.24 (dd, J = 14.5, 10.4 Hz, 1H). ^{13}C NMR (126 MHz, DMSO-d_6) δ 172.17, 163.35, 161.18, 147.20, 147.09, 138.86, 133.43, 132.32, 132.03, 130.22, 128.18, 124.43, 123.93, 121.78, 121.58, 118.43, 115.73, 52.10, 32.78. MS (ESI−): 414.3 [M − 1].

*Synthesis of 2-(4-Butylbenzamido)-3-(2-oxo-1,2-dihydroquinolin-4-yl)propanoic Acid (**14**).* The compound **14** was prepared by using 2-amino-3-(2-oxo-1,2-dihydroquinolin-4-yl)propanoic acid hydrochloride, NaOH, and 4-*n*-butylbenzoyl chloride as described in the above general procedure. ^{1}H NMR (500 MHz, DMSO-d_6) δ 12.98 (s, 1H), 11.64 (s, 1H), 8.71 (d, J = 8.3 Hz, 1H), 7.84 (d, J = 8.1 Hz, 1H), 7.72 (d, J = 8.1 Hz, 2H), 7.53−7.47 (m, 1H), 7.34−7.20 (m, 4H), 6.47 (s, 1H), 4.98−4.29 (m, 1H), 3.49 (dd, J = 14.4, 3.8 Hz, 1H), 3.24 (dd, J = 14.4, 10.8 Hz, 1H), 2.62 (t, J = 7.7 Hz, 2H), 1.60−1.51 (m, 2H), 1.29 (h, J = 7.4 Hz, 2H), 0.89 (t, J = 7.4 Hz, 3H). ^{13}C NMR (126 MHz, DMSO-d_6) δ 172.84, 166.33, 161.31, 147.40, 146.20, 138.95, 131.15, 130.27, 128.16, 127.34, 123.99, 121.88, 121.71, 118.53, 115.83, 51.72, 34.60, 32.85, 32.82, 21.67, 13.72. MS (ESI+): 393.4 [M + 1].

*Synthesis of 2-(4-Hexylbenzamido)-3-(2-oxo-1,2-dihydroquinolin-4-yl)propanoic Acid (**15**).* The compound **15** was prepared by using 2-amino-3-(2-oxo-1,2-dihydroquinolin-4-yl)propanoic acid hydrochloride, NaOH, and 4-*n*-hexylbenzoyl chloride as described in the above general procedure. ^{1}H NMR (500 MHz, DMSO-d_6) δ 12.98 (s, 1H), 11.64 (s, 1H), 8.72 (d, J = 8.2 Hz, 1H), 7.84 (d, J = 7.9 Hz, 1H), 7.76−7.66 (m, 2H), 7.53−7.48 (m, 1H), 7.34−7.21 (m, 4H), 6.47 (s, 1H), 4.80−4.70 (m, 1H), 3.48 (dd, J = 14.4, 3.8 Hz, 1H), 3.24 (dd, J = 14.4, 10.8 Hz, 1H), 2.61 (t, J = 7.6 Hz, 2H), 1.61−1.51 (m, 2H), 1.29−1.22 (m, 6H), 0.88−0.81 (m, 3H). ^{13}C NMR (126 MHz, DMSO-d_6) δ 172.84, 166.34, 161.30, 147.39, 146.22, 138.95, 131.14, 130.27, 128.16, 127.34, 123.99, 121.88, 121.71, 118.53, 115.82, 51.72, 34.92, 32.85, 31.04, 30.62, 28.23, 22.02, 13.92. MS (ESI+): 421.4 [M + 1].

*Synthesis of 2-(3-(4-Chlorophenyl)ureido)-3-(2-oxo-1,2-dihydroquinolin-4-yl)propanoic Acid (**32**).* The compound **32** was prepared by using 2-amino-3-(2-oxo-1,2-dihydroquinolin-4-yl)propanoic acid hydrochloride, NaOH, and 4-chlorophenylisocyanate as described in the above general procedure. ^{1}H NMR (301 MHz, DMSO) δ 13.12 (s, 1H), 11.66 (s, 1H), 8.95 (s, 1H), 7.87 (d, J = 8.1 Hz, 1H), 7.49 (t, J = 7.5 Hz, 1H), 7.43−7.10 (m, 6H), 6.69 (s, 1H), 6.39 (s, 1H), 4.47 (br, 1H), 3.33 (water + geminal H; m,1H) 3.02−3.20 (m, 1H). ^{13}C NMR (76 MHz, DMSO) δ 173.72, 161.83, 155.14, 147.86, 139.68, 139.40, 130.67, 128.93, 125.13, 124.81, 122.42, 122.21, 119.63, 119.36, 116.18, 34.85. MS (ESI+): 386.2 [M + 1].

*Synthesis of 2-(3-(3,5-Dichlorophenyl)ureido)-3-(2-oxo-1,2-dihydroquinolin-4-yl)propanoic Acid (**33**).* The compound **33** was prepared by using 2-amino-3-(2-oxo-1,2-dihydroquinolin-4-yl)-propanoic acid hydrochloride, NaOH, and 3,5-chlorophenylisocyanate as described in the above general procedure. ^{1}H NMR (301 MHz, DMSO) δ 11.59 (s, 1H), 9.88 (s, 1H), 7.96 (d, J = 8.1 Hz, 1H), 7.51−7.40 (m, 3H), 7.29 (d, J = 8.1 Hz, 1H), 7.16 (t, J = 7.6 Hz, 1H), 7.10 (s, 1H), 7.00 (t, J = 1.8 Hz, 1H), 6.37 (s, 1H), 4.30−4.20 (m, 1H), 3.35−3.24 (m, 1H), 3.08 (dd, J = 13.8, 7.1 Hz, 1H). ^{13}C NMR (76 MHz, DMSO) δ 161.99, 154.99, 148.96, 143.84, 139.32, 134.35, 130.35, 125.13, 122.17, 121.98, 120.11, 119.87, 116.00, 115.87, 54.47, 35.79. MS (ESI−): 418.3 [M − 1].

General Procedure for the Synthesis of 2-Amino-3-(2-oxo-1,2-dihydroquinolin-4-yl)propanoic Acid Imide Derivatives. A mixture of 2-amino-3-(2-oxo-1,2-dihydroquinolin-4-yl)propanoic acid hydrochloride(269 mg, 1 mmol) and imide derivative (1 mmol) in DMF (3.0 mL) was stirred at 100 oC overnight. The reaction mixture was cooled to room temperature, and water was added. The precipitated product was filtered and washed with water and ether. The crude product was then purified by recrystallization using an appropriate solvent system (ethanol or ethanol−water).

https://doi.org/10.1021/acs.jmedchem.3c01763
J. Med. Chem. 2024, 67, 1949−1960

*Synthesis of 2-(1,3-Dioxoisoindolin-2-yl)-3-(2-oxo-1,2-dihydroquinolin-4-yl)propanoic Acid (**24**).* The compound **24** was prepared by using 2-amino-3-(2-oxo-1,2-dihydroquinolin-4-yl)propanoic acid hydrochloride and phthalic anhydride as described in the above procedure. ^{1}H NMR (500 MHz, DMSO-d_6) δ 13.56 (s, 1H), 11.61 (s, 1H), 7.90−7.84 (m, 4H), 7.80 (d, J = 8.1 Hz, 1H), 7.50−7.46 (m, 1H), 7.28 (dd, J = 8.2, 1.2 Hz, 1H), 7.21−7.15 (m, 1H), 6.26 (s, 1H), 5.18 (dd, J = 11.1, 4.3 Hz, 1H), 3.74 (dd, J = 14.6, 4.3 Hz, 1H), 3.51 (dd, J = 14.7, 11.0 Hz, 1H). ^{13}C NMR (126 MHz, DMSO-d_6) δ 169.50, 166.98, 160.97, 147.10, 138.75, 134.97, 130.61, 130.32, 123.95, 123.44, 121.79, 121.59, 118.13, 115.68, 50.87, 30.59. MS (ESI +): 363.2 [M + 1].

*Synthesis of 2-(5-Chloro-1,3-dioxoisoindolin-2-yl)-3-(2-oxo-1,2-dihydroquinolin-4-yl)propanoic Acid (**25**).* The compound **25** was prepared by using 2-amino-3-(2-oxo-1,2-dihydroquinolin-4-yl)-propanoic acid hydrochloride and 4-chlorophthalic anhydride as described in the above procedure. ^{1}H NMR (500 MHz, DMSO-d_6) δ 13.60 (s, 1H), 11.61 (s, 1H), 7.98 (d, J = 1.8 Hz, 1H), 7.94−7.86 (m, 2H), 7.79 (d, J = 8.1 Hz, 1H), 7.48 (t, J = 7.7 Hz, 1H), 7.28 (d, J = 8.2 Hz, 1H), 7.18 (t, J = 7.6 Hz, 1H), 6.27 (s, 1H), 5.18 (dd, J = 11.0, 4.4 Hz, 1H), 3.74 (dd, J = 14.7, 4.3 Hz, 1H), 3.48 (dd, J = 14.7, 10.8 Hz, 1H). ^{13}C NMR (126 MHz, DMSO-d_6) δ 169.31, 166.07, 165.73, 160.97, 146.99, 139.90, 138.77, 134.82, 132.52, 130.32, 129.09, 125.23, 123.94, 123.71, 121.79, 121.65, 118.11, 115.69, 51.09, 30.58. MS (ESI+): 397.2 [M + 1].

*Synthesis of Methyl 2-(4-Methylbenzamido)-3-(2-oxo-1,2-dihydroquinolin-4-yl)propanoate (**29**).* 2-(4-methylbenzamido)-3-(2-oxo-1,2-dihydroquinolin-4-yl)propanoic acid (207, 0.5 mmol) was suspended in anhydrous methanol (3.0 mL). The suspension was cooled to 0 °C, and then, thionlyl chloride (2 equiv) was added dropwise. The resulting mixture was stirred at room temperature overnight, and the solvent was removed under reduced pressure. The crude product was recrystallized from ethanol/ethyl acetate to give a white solid of **29**. ^{1}H NMR (500 MHz, DMSO-d_6) δ 11.65 (s, 1H), 8.85 (d, J = 7.9 Hz, 1H), 7.82 (d, J = 8.0 Hz, 1H), 7.71 (d, J = 8.2 Hz, 2H), 7.47−7.53 (m, 1H), 7.35−7.19 (m, 4H), 6.45 (s, 1H), 4.76−4.83 (m, 1H), 3.68 (s, 3H), 3.47 (dd, J = 14.0, 4.7 Hz, 3H), 3.28 (dd, J = 14.4, 10.5 Hz, 1H), 2.35 (s, 3H). ^{13}C NMR (126 MHz, DMSO-d_6) δ 171.69, 166.23, 161.17, 146.97, 141.49, 138.84, 130.53, 130.22, 128.76, 127.26, 123.89, 121.79, 121.72, 118.39, 115.73, 52.12, 51.71, 32.51, 20.86. MS (ESI+): 365.3 [M + 1].

*Synthesis of 2-((1-Carboxy-2-(2-oxo-1,2-dihydroquinolin-4-yl)-ethyl)carbamoyl)benzoic Acid (**22**).* A mixture of 2-amino-3-(2-oxo-1,2-dihydroquinolin-4-yl)propanoic acid hydrochloride (269 mg, 1 mmol) and imide derivative (phthalic anhydride, 1 mmol) in the DMF-pyridine mixture (6.0 mL) was stirred at room temperature overnight. The reaction mixture was diluted with water, and the precipitate was collected by filtration, washed with water, methanol and ether. The crude product was purified by recrystallization from ethanol. ^{1}H NMR (500 MHz, DMSO-d_6) δ 12.89 (s, 1H), 11.65 (s, 1H), 8.82 (d, J = 8.0 Hz, 1H), 7.86 (d, J = 8.0 Hz, 1H), 7.74 (dd, J = 7.5, 1.5 Hz, 1H), 7.61−7.48 (m, 3H), 7.32−7.39 (m, 2H), 7.22−7.27 (m, 1H), 6.48 (s, 1H), 4.62−4.70 (m, 1H), 3.40−3.35 (m, 1H), 3.18 (dd, J = 14.3, 8.9 Hz, 1H). ^{13}C NMR (126 MHz, DMSO-d_6) δ 172.28, 168.14, 167.74, 161.27, 146.89, 138.91, 137.28, 131.02, 130.88, 130.13, 129.39, 128.97, 127.52, 123.94, 121.90, 121.77, 118.48, 115.73, 51.72, 33.29. MS (ESI−): 379.3 [M − 1].

*Synthesis of 2,2′-((4,4′-Oxybis(benzoyl))bis(azanediyl))bis(3-(2-oxo-1,2-dihydroquinolin-4-yl)propanoic Acid) (**28**).* To a stirred solution of 2-amino-3-(2-oxo-1,2-dihydroquinolin-4-yl)propanoic acid hydrochloride(1.35 g, 5 mmol) and sodium hydroxide (600 mg, 15 mmol) in water (5.0 mL) at 0 °C was added a solution of 4,4′-oxidibenzoyl chloride (295 mg) in acetone (2.5 mL). The resulting mixture was stirred at room temperature overnight. The formed precipitate was filtered and washed with water, methanol, and ethyl acetate. The product was suspended in 2 N HCl and stirred for 1 h. The white solid was collected by filtration and washed with water and methanol to give the title compound **28** as a mixture of isomers. ^{1}H NMR (500 MHz, DMSO-d_6; note that, while the compound is a dimer the data is reported as a monomer) δ 11.68 (s, 1H), 8.82 (d, J = 8.2 Hz, 1H), 7.93−7.81 (m, 3H), 7.55−7.48 (m, 1H), 7.33 (d, J = 8.1 Hz, 1H), 7.28−7.22 m, 1H), 7.17−7.09 (m, 2H), 6.47 (s, 1H), 4.80−4.69 (m, 1H), 3.50 (dd, J = 14.4, 3.8 Hz, 1H), 3.26 (dd, J = 14.5, 10.8 Hz, 1H). ^{13}C NMR (126 MHz, DMSO-d_6) δ 172.69, 165.52, 161.23, 158.51, 147.36, 138.84, 130.21, 129.58, 129.01, 123.91, 121.84, 121.53, 118.45, 118.31, 115.76, 51.71, 32.73. MS (ESI+): 687.5 [M + 1].

*Synthesis of 4-Chloro-N-(1-(hydroxyamino)-1-oxo-3-(2-oxo-1,2-dihydroquinolin-4-yl)propan-2-yl)benzamide (**30**).* 2-(4-chlorobenzamido)-3-(2-oxo-1,2-dihydroquinolin-4-yl)propanoic acid (rebamipide, 371 mg, 1 mmol) was dissolved in DMF and cooled to 0 °C. To this mixture were then successively added EDCI (2 mmol), HOAt (2 mmol), and *N*-methylmorpholine (2 mmol) under nitrogen atmosphere. The solution was stirred at 0 °C for 15 min and then at room temperature for 1 h. After this time, 50% hydroxylamine (10 mmol) was added. The mixture was stirred at room temperature for 5h, and the solution was diluted with water. The formed precipitate was filtered, washed with water, and purified by recrystallization (ethanol). ^{1}H NMR (500 MHz, DMSO-d_6) δ 11.61 (s, 1H), 10.97 (s, 1H), 8.99 (s, 1H), 8.84 (d, J = 8.4 Hz, 1H), 7.91 (d, J = 8.1 Hz, 1H), 7.88−7.80 (m, 2H), 7.56−7.46 (m, 3H), 7.30 (d, J = 8.1 Hz, 1H), 7.20−7.26 (m, 1H), 6.48 (s, 1H), 4.72−4.80 (m, 1H), 3.28−3.36 (m, 1H, buried under water peak), 3.19 (dd, J = 14.3, 10.1 Hz, 1H). ^{13}C NMR (126 MHz, DMSO-d_6) δ 167.10, 165.15, 161.21, 147.07, 138.79, 136.13, 132.41, 130.12, 129.33, 128.16, 124.36, 121.75, 121.71, 118.52, 115.57, 50.35, 33.69. MS (ESI−): 384.2 [M − 1].

*Synthesis of N-(4-Methylbenzoyl)-S-((2-oxo-1,2-dihydroquinolin-4-yl)methyl)-L-cysteine (**34**).* To a stirred solution of L-cysteine (121 mg, 1 mmol) and sodium hydroxide (160 mg, 4 mmol) in water (2.0 mL) was added a solution of 4-(bromomethyl)quinolin-2(1H)-one (238 mg 1 mmol) in acetone (2.0 mL). The resulting mixture was stirred at room temperature for 5 h. After this time, a solution of 4-methylbenzoyl chloride (1 mmol) in acetone (2 mL) was added dropwise, and the resulting mixture was stirred for another 5h. The reaction mixture was diluted with water and acidified with 2 N HCl. The formed precipitate was collected by filtration, washed with water, and purified by recrystallization from ethanol. ^{1}H NMR (500 MHz, DMSO-d_6) δ 11.69 (s, 1H), 8.69 (d, J = 8.1 Hz, 1H), 7.76−7.81 (m, 3H), 7.48 (t, J = 7.7 Hz, 1H), 7.25−7.34 (m, 3H), 7.13 (t, J = 7.6 Hz, 1H), 6.51 (s, 1H), 4.71−4.58 (m, 1H), 4.08−3.90 (m, 2H), 3.04 (dd, J = 13.6, 4.7 Hz, 1H), 2.93 (dd, J = 13.7, 9.8 Hz, 1H), 2.36 (s, 3H). ^{13}C NMR (126 MHz, DMSO-d_6) δ 172.09, 166.15, 161.19, 146.91, 141.27, 139.16, 130.92, 130.22, 128.72, 127.32, 125.00, 121.37, 121.13, 117.66, 115.55, 52.06, 32.49, 31.72, 20.88. MS (ESI+): 397.3 [M + 1].

Visualization Software Used. Chemical structures (Figures 1A, 3 and 7) were made using ChemDraw 22 (PerkinElmer), protein structure images (Figure 4) were made using PyMol 2.3.3 (Schrodinger), the APBS plugin[23] in PyMol was used to generate the electrostatic surface (Figure 4A), and graphs (Figures 1, 2, and 5) were generated using KaleidaGraph v4.03 (Synergy Software).

■ ASSOCIATED CONTENT

Data Availability Statement

The coordinate files and experimental data for the two structures described herein are freely available through the protein data bank (www.rcsb.org) with identifiers 8U5M and 8U7E. Coordinate files and reflection data of structures described in this manuscript, PDB IDs 8U5M (Sts with rebamipide, 1) and 8U7E (Sts with 11), will be released upon article publication.

Supporting Information

The Supporting Information is available free of charge at https://pubs.acs.org/doi/10.1021/acs.jmedchem.3c01763.

Inhibition data with error values; data collection and refinement statistics; competitive inhibition by rebamipide; rebamipide does not inhibit the Sts-1$_{HP}$ W505L

https://doi.org/10.1021/acs.jmedchem.3c01763
J. Med. Chem. 2024, 67, 1949−1960

mutant; structure of rebamipide bound to Sts-1_{HP} showing electron density; structure of compound 11 (ethyl derivative) bound to Sts-1_{HP}; predicted low energy conformer of rebamipide; inhibition of PTP-1B; inhibition of SHP-1B; inhibition of Sts-2_{HP}; features of Sts-1_{HP} near the *para*-position of the phenyl group; and HPLC traces of representative compounds (PDF)

Molecular formula strings; coordinate files, and reflection data (CSV)

AUTHOR INFORMATION

Corresponding Author

Jarrod B. French − *The Hormel Institute, University of Minnesota, Austin, Minnesota 55912, United States;* orcid.org/0000-0002-6762-1309; Phone: +1 507-437-9637; Email: jfrench@umn.edu

Authors

Faisal Aziz − *The Hormel Institute, University of Minnesota, Austin, Minnesota 55912, United States*

Kanamata Reddy − *The Hormel Institute, University of Minnesota, Austin, Minnesota 55912, United States*

Virneliz Fernandez Vega − *Department of Molecular Medicine, The Herbert Wertheim UF Scripps Institute, Jupiter, Florida 33458, United States*

Raja Dey − *The Hormel Institute, University of Minnesota, Austin, Minnesota 55912, United States*

Katherine A. Hicks − *Department of Chemistry, State University of New York at Cortland, Cortland, New York 13045, United States;* orcid.org/0000-0002-1474-1067

Sumitha Rao − *Department of Molecular Medicine, The Herbert Wertheim UF Scripps Institute, Jupiter, Florida 33458, United States*

Luis Ortiz Jordan − *Department of Molecular Medicine, The Herbert Wertheim UF Scripps Institute, Jupiter, Florida 33458, United States*

Emery Smith − *Department of Molecular Medicine, The Herbert Wertheim UF Scripps Institute, Jupiter, Florida 33458, United States*

Justin Shumate − *Department of Molecular Medicine, The Herbert Wertheim UF Scripps Institute, Jupiter, Florida 33458, United States*

Louis Scampavia − *Department of Molecular Medicine, The Herbert Wertheim UF Scripps Institute, Jupiter, Florida 33458, United States*

Nicholas Carpino − *Department of Microbiology and Immunology, Stony Brook University, Stony Brook, New York 11790, United States*

Timothy P. Spicer − *Department of Molecular Medicine, The Herbert Wertheim UF Scripps Institute, Jupiter, Florida 33458, United States*

Complete contact information is available at: https://pubs.acs.org/10.1021/acs.jmedchem.3c01763

Author Contributions

[⊥]F.A. and K.R. contributed equally to this work.

Funding

This work was supported by the National Institute of Allergy and Infectious Diseases of the National Institutes of Health, Department of Health and Human Services, under grant number R01AI141592 (N.K., J.B.F., L.S.). N.K. and J.B.F. would also like to acknowledge Stony Brook University, Department of Microbiology and Immunology, and The Hormel Institute, respectively, for additional support. Work at SUNY Cortland was supported by the National Science Foundation grant 1817633.

Notes

The authors declare no competing financial interest.

ACKNOWLEDGMENTS

The authors would like to thank Andrew Roering and Ivan Vuckovic from SUNY Cortland and the Mayo Clinic Metabolomics Core, respectively, for assistance with NMR data collection.

ABBREVIATIONS

HP:histidine phosphatase; PDE:phosphodiesterase; PGM:phosphoglycerate mutase; PTP:protein tyrosine phosphatase; SH3:Src-homology 3 domain; Sts:suppressor of T cell signaling; Sts-1_{HP}:histidine phosphatase of Sts-1; $Sts^{-/-}$:Sts double knockout mouse strain; UBA:ubiquitin association domain

REFERENCES

(1) Tsygankov, A. Y. TULA-family proteins: Jacks of many trades and then some. *J. Cell. Physiol.* **2019**, *234* (1), 274−288.

(2) (a) Carpino, N.; Chen, Y.; Nassar, N.; Oh, H. W. The Sts proteins target tyrosine phosphorylated, ubiquitinated proteins within TCR signaling pathways. *Molecular immunology* **2009**, *46* (16), 3224−31. (b) Carpino, N.; Turner, S.; Mekala, D.; Takahashi, Y.; Zang, H.; Geiger, T. L.; Doherty, P.; Ihle, J. N. Regulation of ZAP-70 activation and TCR signaling by two related proteins, Sts-1 and Sts-2. *Immunity* **2004**, *20* (1), 37−46. (c) Luis, B. S.; Carpino, N. Insights into the suppressor of T-cell receptor (TCR) signaling-1 (Sts-1)-mediated regulation of TCR signaling through the use of novel substrate-trapping Sts-1 phosphatase variants. *FEBS J.* **2014**, *281* (3), 696−707. (d) Tsygankov, A. Y. TULA proteins as signaling regulators. *Cellular signalling* **2020**, *65*, No. 109424.

(3) (a) Naseem, S.; Frank, D.; Konopka, J. B.; Carpino, N. Protection from systemic Candida albicans infection by inactivation of the Sts phosphatases. *Infection and immunity* **2015**, *83* (2), 637−45. (b) Parashar, K.; Kopping, E.; Frank, D.; Sampath, V.; Thanassi, D. G.; Carpino, N. Increased Resistance to Intradermal Francisella tularensis LVS Infection by Inactivation of the Sts Phosphatases. *Infect. Immun.* **2017**, *85* (9), e00406-17.

(4) (a) Carpino, N.; Naseem, S.; Frank, D. M.; Konopka, J. B. Modulating Host Signaling Pathways to Promote Resistance to Infection by Candida albicans. *Front. Cell. Infect. Microbiol.* **2017**, *7*, 481. (b) Newman, T. N.; Liverani, E.; Ivanova, E.; Russo, G. L.; Carpino, N.; Ganea, D.; Safadi, F.; Kunapuli, S. P.; Tsygankov, A. Y. Members of the novel UBASH3/STS/TULA family of cellular regulators suppress T-cell-driven inflammatory responses in vivo. *Immunology and cell biology* **2014**, *92* (10), 837−50.

(5) (a) Mikhailik, A.; Ford, B.; Keller, J.; Chen, Y.; Nassar, N.; Carpino, N. A phosphatase activity of Sts-1 contributes to the suppression of TCR signaling. *Mol. Cell* **2007**, *27* (3), 486−97. (b) San Luis, B.; Sondgeroth, B.; Nassar, N.; Carpino, N. Sts-2 is a phosphatase that negatively regulates zeta-associated protein (ZAP)-70 and T cell receptor signaling pathways. *J. Biol. Chem.* **2011**, *286* (18), 15943−54. (c) Zhou, W.; Yin, Y.; Weinheimer, A. S.; Kaur, N.; Carpino, N.; French, J. B. Structural and Functional Characterization of the Histidine Phosphatase Domains of Human Sts-1 and Sts-2. *Biochemistry* **2017**, *56* (35), 4637−4645.

(6) Yin, Y.; Frank, D.; Zhou, W.; Kaur, N.; French, J. B.; Carpino, N. An unexpected 2-histidine phosphoesterase activity of suppressor of T-cell receptor signaling protein 1 contributes to the suppression of cell signaling. *J. Biol. Chem.* **2020**, *295* (25), 8514−8523.

(7) (a) Agrawal, R.; Carpino, N.; Tsygankov, A. TULA proteins regulate activity of the protein tyrosine kinase Syk. *J. Cell. biochem.* **2008**, *104* (3), 953−64. (b) Thomas, D. H.; Getz, T. M.; Newman, T. N.; Dangelmaier, C. A.; Carpino, N.; Kunapuli, S. P.; Tsygankov, A. Y.; Daniel, J. L. A novel histidine tyrosine phosphatase, TULA-2, associates with Syk and negatively regulates GPVI signaling in platelets. *Blood* **2010**, *116* (14), 2570−8.

(8) (a) Chen, Y.; Jakoncic, J.; Carpino, N.; Nassar, N. Structural and functional characterization of the 2H-phosphatase domain of Sts-2 reveals an acid-dependent phosphatase activity. *Biochemistry* **2009**, *48* (8), 1681−90. (b) Chen, Y.; Jakoncic, J.; Wang, J.; Zheng, X.; Carpino, N.; Nassar, N. Structural and functional characterization of the c-terminal domain of the ecdysteroid phosphate phosphatase from bombyx mori reveals a new enzymatic activity. *Biochemistry* **2008**, *47* (46), 12135−45.

(9) (a) Bond, C. S.; White, M. F.; Hunter, W. N. High resolution structure of the phosphohistidine-activated form of Escherichia coli cofactor-dependent phosphoglycerate mutase. *J. Biol. Chem.* **2001**, *276* (5), 3247−53. (b) Bond, C. S.; White, M. F.; Hunter, W. N. Mechanistic implications for Escherichia coli cofactor-dependent phosphoglycerate mutase based on the high-resolution crystal structure of a vanadate complex. *J. Mol. Biol.* **2002**, *316* (5), 1071−81. (c) Rigden, D. J. The histidine phosphatase superfamily: structure and function. *biochem. J.* **2008**, *409* (2), 333−48. (d) Zheng, Q.; Jiang, D.; Zhang, W.; Zhang, Q.; Zhao, Q.; Jin, J.; Li, X.; Yang, H.; Bartlam, M.; Shaw, N.; Zhou, W.; Rao, Z. Mechanism of dephosphorylation of glucosyl-3-phosphoglycerate by a histidine phosphatase. *J. Biol. Chem.* **2014**, *289* (31), 21242−51.

(10) (a) Li, N.; Wang, Y.; Wang, A.; Zhang, J.; Jia, C.; Yu, C.; Song, Z.; Wang, S.; Liu, L.; Yi, J.; Bao, Y.; Huang, Y.; Sun, L. STS1 and STS2 Phosphatase Inhibitor Baicalein Enhances the Expansion of Hematopoietic and Progenitor Stem Cells and Alleviates 5-Fluorouracil-Induced Myelosuppression *Int. J. Mol. Sci.* **2023**, *24* (3), 2987, DOI: 10.3390/ijms24032987. (b) Zhou, W.; Yin, Y.; Smith, E.; Chou, J.; Shumate, J.; Scampavia, L.; Spicer, T. P.; Carpino, N.; French, J. B. Discovery and Characterization of Two Classes of Selective Inhibitors of the Suppressor of the TCR Signaling Family of Proteins. *ACS infectious diseases* **2019**, *5* (2), 250−259.

(11) Baillargeon, P.; Fernandez-Vega, V.; Sridharan, B. P.; Brown, S.; Griffin, P. R.; Rosen, H.; Cravatt, B.; Scampavia, L.; Spicer, T. P. The Scripps Molecular Screening Center and Translational Research Institute. *SLAS discovery: advancing life sciences R & D* **2019**, *24* (3), 386−397.

(12) Hellmuth, K.; Grosskopf, S.; Lum, C. T.; Wurtele, M.; Roder, N.; von Kries, J. P.; Rosario, M.; Rademann, J.; Birchmeier, W. Specific inhibitors of the protein tyrosine phosphatase Shp2 identified by high-throughput docking. *Proc. Natl. Acad. Sci. U.S.A.* **2008**, *105* (20), 7275−80.

(13) Baell, J. B.; Holloway, G. A. New substructure filters for removal of pan assay interference compounds (PAINS) from screening libraries and for their exclusion in bioassays. *J. Med. Chem.* **2010**, *53* (7), 2719−40.

(14) (a) Arakawa, T.; Kobayashi, K.; Yoshikawa, T.; Tarnawski, A. Rebamipide: overview of its mechanisms of action and efficacy in mucosal protection and ulcer healing. *Dig. Dis. Sci.* **1998**, *43*, 5S−13S. (b) Arakawa, T.; Watanabe, T.; Fukuda, T.; Yamasaki, K.; Kobayashi, K. Rebamipide, novel prostaglandin-inducer accelerates healing and reduces relapse of acetic acid-induced rat gastric ulcer. Comparison with cimetidine. *Digestive diseases and sciences* **1995**, *40* (11), 2469−72. (c) Takumida, M.; Anniko, M. Radical scavengers for elderly patients with age-related hearing loss. *Acta oto-laryngologica* **2009**, *129* (1), 36−44. (d) Tarnawski, A.; Pai, R.; Chiou, S. K.; Chai, J.; Chu, E. C. Rebamipide inhibits gastric cancer growth by targeting survivin and Aurora-B. *biochem. Biophys. Res. Commun.* **2005**, *334* (1), 207−12. (e) Tarnawski, A. S.; Chai, J.; Pai, R.; Chiou, S. K. Rebamipide activates genes encoding angiogenic growth factors and Cox2 and stimulates angiogenesis: a key to its ulcer healing action? *Digestive diseases and sciences* **2004**, *49* (2), 202−9. (f) Terano, A.; Arakawa, T.; Sugiyama, T.; Suzuki, H.; Joh, T.; Yoshikawa, T.; Higuchi, K.; Haruma, K.; Murakami, K.; Kobayashi, K.; Rebamipide Clinical Study, G. Rebamipide, a gastro-protective and anti-inflammatory drug, promotes gastric ulcer healing following eradication therapy for Helicobacter pylori in a Japanese population: a randomized, double-blind, placebo-controlled trial. *J. Gastroenterol.* **2007**, *42* (8), 690−693.

(15) (a) Kim, S.; Bolton, E. E.; Bryant, S. H. Similar compounds versus similar conformers: complementarity between PubChem 2-D and 3-D neighboring sets. *J. Cheminf.* **2016**, *8*, 62. (b) Kim, S.; Chen, J.; Cheng, T.; Gindulyte, A.; He, J.; He, S.; Li, Q.; Shoemaker, B. A.; Thiessen, P. A.; Yu, B.; Zaslavsky, L.; Zhang, J.; Bolton, E. E. PubChem 2023 update. *Nucleic Acids Res.* **2023**, *51* (D1), D1373−D1380.

(16) (a) Okawa, S.; Sumimoto, Y.; Masuda, K.; Ogawara, K. I.; Maruyama, M.; Higaki, K. Improvement of lipid solubility and oral bioavailability of a poorly water- and poorly lipid-soluble drug, rebamipide, by utilizing its counter ion and SNEDDS preparation. *European journal of pharmaceutical sciences: official journal of the European Federation for Pharmaceutical Sciences* **2021**, *159*, No. 105721. (b) Shi, Y.; Zou, M.; An, Y.; Ji, Z.; Gao, P.; Cheng, G. A potent preparation method combining neutralization with microfluidization for rebamipide nanosuspensions and its in vivo evaluation. *Drug Dev. Ind. Pharm.* **2013**, *39* (7), 996−1004.

(17) (a) Fernandez-Vega, V.; Hou, S.; Plenker, D.; Tiriac, H.; Baillargeon, P.; Shumate, J.; Scampavia, L.; Seldin, J.; Souza, G. R.; Tuveson, D. A.; Spicer, T. P. Lead identification using 3D models of pancreatic cancer. *SLAS discovery: advancing life sciences R & D* **2022**, *27* (3), 159−166. (b) Otsuka, Y.; Airola, M. V.; Choi, Y. M.; Coant, N.; Snider, J.; Cariello, C.; Saied, E. M.; Arenz, C.; Bannister, T.; Rahaim, R., Jr; Hannun, Y. A.; Shumate, J.; Scampavia, L.; Haley, J. D.; Spicer, T. P. Identification of Small-Molecule Inhibitors of Neutral Ceramidase (nCDase) via Target-Based High-Throughput Screening. *SLAS discovery: advancing life sciences R & D* **2021**, *26* (1), 113−121.

(18) Zhang, J. H.; Chung, T. D.; Oldenburg, K. R. A Simple Statistical Parameter for Use in Evaluation and Validation of High Throughput Screening Assays. *Journal of biomolecular screening* **1999**, *4* (2), 67−73.

(19) (a) Evans, P. Scaling and assessment of data quality. *Acta Crystallogr., Sect. D: Biol. Crystallogr.* **2006**, *62* (Pt 1), 72−82. (b) Kabsch, W. Xds. *Acta Crystallogr., Sect. D: Biol. Crystallogr.* **2010**, *66* (Pt 2), 125−132. (c) Sauter, N. K.; Poon, B. K. Autoindexing with outlier rejection and identification of superimposed lattices. *J. Appl. Crystallogr.* **2010**, *43* (Pt 3), 611−616.

(20) Vagin, A.; Teplyakov, A. Molecular replacement with MOLREP. *Acta Crystallogr., Sect. D: Biol. Crystallogr.* **2010**, *66* (Pt 1), 22−25.

(21) (a) Emsley, P.; Cowtan, K. Coot: model-building tools for molecular graphics. *Acta Crystallogr., Sect. D: Biol. Crystallogr.* **2004**, *60* (Pt 12 Pt 1), 2126−2132. (b) Murshudov, G. N.; Vagin, A. A.; Dodson, E. J. Refinement of macromolecular structures by the maximum-likelihood method. *Acta Crystallogr., Sect. D: Biol. Crystallogr.* **1997**, *53* (Pt 3), 240−255.

(22) (a) Liebschner, D.; Afonine, P. V.; Baker, M. L.; Bunkoczi, G.; Chen, V. B.; Croll, T. I.; Hintze, B.; Hung, L. W.; Jain, S.; McCoy, A. J.; Moriarty, N. W.; Oeffner, R. D.; Poon, B. K.; Prisant, M. G.; Read, R. J.; Richardson, J. S.; Richardson, D. C.; Sammito, M. D.; Sobolev, O. V.; Stockwell, D. H.; Terwilliger, T. C.; Urzhumtsev, A. G.; Videau, L. L.; Williams, C. J.; Adams, P. D. Macromolecular structure determination using X-rays, neutrons and electrons: recent developments in PHENIX. *Acta Crystallogr., Sect. D: Struct. Biol.* **2019**, *75* (Pt 10), 861−877. (b) Moriarty, N. W.; Grosse-Kunstleve, R. W.; Adams, P. D. electronic Ligand Builder and Optimization Workbench (eLBOW): a tool for ligand coordinate and restraint generation. *Acta Crystallogr., Sect. D: Biol. Crystallogr.* **2009**, *65* (Pt 10), 1074−1080.

(23) Baker, N. A.; Sept, D.; Joseph, S.; Holst, M. J.; McCammon, J. A. Electrostatics of nanosystems: application to microtubules and the ribosome. *Proc. Natl. Acad. Sci. U.S.A.* **2001**, *98* (18), 10037−41.